

Aus der Klinik für Frauenheilkund und Geburtshilfe
der Medizinischen Fakultät Charité – Universitätsmedizin Berlin

DISSERTATION

Epigenetic Quantification of Tumor-Infiltrating
T-lymphocytes in Epithelial Ovarian Tumors

zur Erlangung des akademischen Grades
Doctor medicinae (Dr. med.)

vorgelegt der Medizinischen Fakultät
Charité – Universitätsmedizin Berlin

von

Ines Isabel Monteiro Vasconcelos
aus Coimbra, Portugal

Promotionsdatum: 22.06.2014

Table of Contents

Abstract (English)	4
Abstract (German)	6
List of Abbreviations in Alphabetical Order	8
Introduction	11
Immunology	11
<i>The innate and the adaptive immune system</i>	11
<i>Tumor immunology – The concept of immunoediting: elimination, equilibrium and escape</i>	12
<i>Immune-privileged (IP) and non-immune privileged (NIP) sites</i>	15
<i>Regulatory T cells and their phenotypic markers – The transcription factor FOXP3</i>	15
<i>Epigenetics and DNA Methylation</i>	17
Epithelial ovarian cancer and borderline ovarian tumors.....	20
<i>Epidemiology, risk Factors, pathogenesis and screening</i>	20
<i>Diagnosis and histopathology</i>	23
<i>Surgical staging and adjuvant treatment</i>	25
Aim	29
<i>Is there a correlation between different cellular ratios of immune tolerance in the tumor microenvironment and the clinical outcome in borderline ovarian tumors and epithelial ovarian cancers?</i>	29
<i>Is there a correlation between peripheral changes in the cellular ratios of immune tolerance and the transcoelomic metastatic pattern in epithelial ovarian cancer?</i>	29
Materials and Methods	32
Tissue samples, patient and data collection.....	32
Histology.....	34
DNA Extraction.....	34
<i>Tissue</i>	34
<i>Blood</i>	35
Sodium bisulfite conversion.....	36
PCR amplification	37
Identifying cell populations	38
Statistical analysis	41
Results	42
Characteristics of the cohort	42
<i>Immune privileged - EOC</i>	42
<i>BOT</i>	43
Tumor infiltrating lymphocytes.....	45
<i>Overall T lymphocytes – CD3 marker</i>	45
<i>Epigenetic analysis of immunoCRIT in NIP and IP tissues</i>	50
<i>Regulatory T cells and immunoCRIT: Ratio of regulatory T cells relative to the percentage of overall T lymphocytes</i>	50
<i>Sub-analysis of IP malignant tissues – LSOC and BOT; Correlation of disease aggressiveness with immunoCRIT in ovarian tissues</i>	52
<i>ImmunoCRIT in peripheral blood in the cohort of patients with ovarian neoplasia</i>	55
<i>Summary of most prominent findings</i>	59
Discussion	60
Characteristics of the cohort	61

Tumor infiltrating lymphocytes.....	62
<i>Overall T lymphocytes – CD3 marker</i>	62
<i>Regulatory T cells – FOXP3 marker</i>	65
<i>Cellular Ratio of Immune Tolerance - Ratio of regulatory T cells relative to the percentage of overall T lymphocytes:</i>	67
<i>immunoCRIT in NIP and IP tissues, non-invasive and invasive BOT, and proposed model for metastatic spread.....</i>	67
<i>ImmunoCRIT in the peripheral blood of patients with ovarian neoplasia and dissemination patterns dependent on NIP vs. IP tissues.....</i>	71
<i>Concluding Remarks.....</i>	74
Literature References	77
Statement of Responsibility	86
Eidesstattliche Versicherung.....	87
Lebenslauf	88
Publikationsliste.....	91
Danksagung.....	92

Abstract (English)

Immunological tolerance is an important determinant for tumor establishment, aggressiveness and metastasizing potential. Ovarian tumors, known to benefit from an immune-privileged (IP) status, spread via transcoelomic routes, whereas involvement of distant organs is a rare event at primary diagnosis (PD). This is contrary to other tumors, usually belonging to non immune-privileged (NIP) sites that preferably spread haematogeneously to distant organs. Here, we use epigenetic-based immune cell quantification to compare the immune status in different benign and malignant tissues, including from NIP and IP sites, as well as blood from healthy donors and cancer patients. In this study, we introduce the “cellular ratio of immune tolerance” (immunoCRIT) as defined by the ratio of regulatory T cells in the overall T-lymphocytes count. ImmunoCRIT was analyzed on 273 benign tissue samples of colorectal, bronchial, renal and ovarian origin as well as in 589 samples from colorectal, bronchial and mammary malignancies as well as borderline ovarian tumors (BOT), early and late stage epithelial ovarian cancer (ESOC and LSOC) at their respective PD. Strong increases of immunoCRIT values in all cancerous tissues and a gradual, highly significant increase strictly dependent on the aggressiveness in ovarian tumors were observed. Concomitantly, a stable immune privilege in malignant ovarian compared to benign and/or malignant NIP tissues is seen. Based on this, we postulated that non-pathological immunoCRIT values observed in peripheral blood of IP-tumor patients are sufficient to contain haematological spread of this tumor. Conversely, NIP-tumors establish high immunoCRIT in an immunological environment equivalent to the bloodstream and thus spread

hematologically. To test this, we analyzed immunoCRIT values in the periphery of 10 ovarian cancer patients beginning at PD through to various recurrences, at which extra-abdominal, hematological metastases frequently occur. We found an incremental, highly significant immunoCRIT increase at disease recurrence compared to PD. In summary, our data suggest a fundamental role of an elevated immunoCRIT as a mediator of tumor aggressiveness and tumor dissemination.

Abstract (German)

Immunologische Toleranz ist ein wichtiger Faktor für die Entstehung, die Aggressivität und das Metastazierungspotenzial von bösartigen Tumoren. Ovarialkarzinome, die von einem privilegierten Immunstatus (IP) profitieren, metastasieren auf peritonealem Weg, während der hämatogene Befall von distanten Organen bei Erstdiagnose selten ist. Dies steht im Gegensatz zu vielen anderen Tumorerkrankungen, die häufig nicht zu den immunprivilegierten (NIP) Tumorerkrankungen gehören und vorrangig haematogen metastasieren. In der vorliegenden Arbeit wenden wir die epigenetikbasierte Immunzellquantifizierung an, um den Immunstatus in verschiedenen gutartigen und bösartigen Geweben, einschließlich IP und NIP Regionen sowie Blut von gesunden Probandinnen und von Patientinnen mit Ovarialkarzinom, zu vergleichen. Wir verwendeten hierfür die „cellular ratio of immune tolerance“ (immunoCRIT), definiert als die Ratio zwischen der Anzahl regulatorischer T-Zellen und der Gesamtzahl der T-Zellen. Die ImmunoCRIT ist in 273 Proben von gutartigem Gewebe kolorektalen, bronchialen, renalen und ovariellen Ursprungs sowie in 589 Proben von kolorektalen und bronchialen Malignomen, von Malignomen der Mamma, von Borderline-Tumoren des Ovars (BOT), von frühen (ESOC) und fortgeschrittenen (LSOC) epithelialen Ovarialkarzinomen bei Erstdiagnose bestimmt worden. Dabei wurde eine Erhöhung der immunoCRIT in allen Malignomen und eine graduierte, hoch-signifikante Erhöhung abhängig von der Aggressivität der ovariellen Neoplasien beobachtet. Dabei lag bei ovariellen Malignomen, gegenüber benignen oder malignen NIP-Geweben, ein stabiler IP-Status vor. Darauf basierend postulieren wir, dass ein nicht-pathologischer immunoCRIT-

Wert im Blut von IP-Tumorpatienten dafür ausreicht, eine hämatogene Metastasierung zu behindern. Im Gegensatz dazu bilden NIP-Tumoren eine hohe immunoCRIT in einer immunologischen Umgebung äquivalent zum Blut aus und metastasieren daher auf hämatogenem Weg. Um das zu überprüfen analysierten wir immunoCRIT-Werte im Blut von 10 Patientinnen mit Ovarialkarzinom Patientinnen beginnend bei Erstdiagnose bis zu mehreren Rezidiven, bei denen extraabdominelle hämatogene Metastasen häufig auftreten. Wir haben eine schrittweise hochsignifikante Zunahme der immunoCRIT bei Rezidiven im Vergleich zum Zeitpunkt der Erstdiagnose beobachtet.

Zusammenfassend lassen die erfassten Daten eine fundamentale Rolle der immunoCRIT als Mediator von Tumoraggressivität und Aussaat vermuten.

List of Abbreviations in Alphabetical Order

ACOG/SGO – American college of obstetrics and gynecology/Society of gynecological oncology

AJCC – American joint cancer committee

ANOVA – Analysis of variance test

BOT – Borderline ovarian tumors

BRAF – V-raf murine sarcoma viral oncogene homolog B1

BRCA 1/2– Breast cancer susceptibility gene 1/2

CA-125 – Cancer antigen 125

CCL22 – C-C motif chemokine 22

CCR4 – C-C motif chemokine receptor 4

CD25 – cluster of differentiation 25

CTLA-4 – Cytotoxic T-Lymphocyte Antigen 4

DAMPs - Damage-associated molecular pattern molecules

DNA – Deoxyribonucleic acid

EOC – Epithelial ovarian cancer

ESOC – Early stage ovarian cancer

FIGO – International federation of gynecology and obstetrics

FOXP3 – Forkhead box P3

fp – forward primer

G1 – Grade 1

G2/3 – Grade 2/3

GITR – Glucocorticoid-induced TNFR family related gene

GOG – Gynecology oncology group

Id-1 – DNA binding protein inhibitor 1

IDO – Indoleamine 2,3-dioxygenase

IFN- γ – Interferon gamma

IgE – Immunoglobulin E
IL-2 – Interleukin 2
IL-2R – Interleukin 2 receptor
immunoCRIT – Cellular ratio of immune tolerance
IP – Immune-privileged
KRAS – V-Ki-ras2 Kirsten rat sarcoma viral oncogene homologue
LION – Lymphadenectomy in ovarian neoplasm trial
LSD - Fisher's least significant difference test
LSOC – Late stage ovarian cancer
MHC – Major histocompatibility complex
MUC16 – Mucin 16
NIP – Non immune-privileged
NK – Natural Killer
OC – Oral contraceptives
OVCAD – Ovarian cancer diagnosis initiative
OR – Odds Ratio
oTL – overall T lymphocytes
PCR – Polymerase chain reaction
PD – Primary diagnose
PFS – Progression free survival
p – probe
qPCR – Real time polymerase chain reaction
RAG-2 – Recombination activating gene 2
ROCA – Risk of ovarian cancer algorithm
QPCR – Real time polymerase chain reaction
rp – reverse primer
SOP – Standard operating procedure
TAH-BSO – Total abdominal hysterectomy with bilateral salpingo-
oophorectomy
TCR-CD3 – T cell receptor - cluster of differentiation 3 complex

TGF- β – Tumor growth factor β

Th1 – T helper cells 1

Th2 – T helper cells 2

Treg – Regulatory T cells

TSDR – Treg- specific demethylated region

VEGF – Vascular endothelial growth factor

Introduction

Immunology

The innate and the adaptive immune system

The main function of the immune system is self/non-self discrimination.¹ This distinction is necessary to protect the organism from invading pathogens and to eliminate modified or altered cells, resulting in two different, but interrelated, forms of immunity: innate and adaptive immunity.

The innate immune system is comprised of anatomical barriers, phagocytes, natural killer (NK) cells and the complement proteins.² It is fully active before a pathogen enters the body, being the first line of defense against invasion³. The adaptive immune response provides the ability to recognize and remember pathogens, and to mount stronger and more specific attacks each time the pathogen is encountered. The predominant cell in the adaptive immune system is the lymphocyte and it is responsible for the humoral and adaptive responses. The humoral immune system is mediated by antibodies, whereas the cell-mediated immune response results from actions of different types of cells, mainly T lymphocytes⁴. The central event in the generation of cell-mediated responses is the activation and clonal expansion of T cells, initiated by the interaction of the TCR-CD3 complex with a processed antigen presented on the surface of an antigen-presenting cell⁵. T lymphocytes are divided into subsets that have regulatory or effector functions. The regulatory T cells (Treg) are a specialized subpopulation of T

cells that act to suppress the activation and expansion of cells from adaptive and innate immunity, therefore hampering immune responses, while effector T cells are involved in the removal of pathogens, damaged or cancerous cells⁶. The main effector cells include the CD4+ helper T lymphocytes and CD8+ cytotoxic T-lymphocytes.

Cytotoxic CD8+ T lymphocytes have lytic capability, while CD4+ T helper cells secrete cytokines that help B cells and cytotoxic T cells in their function⁵. Proliferating helper CD4+ T cells that develop into effector T cells differentiate into two major subtypes of cells known as Th1 and Th2 cells. The Th1 response tends to produce pro-inflammatory cytokines that are responsible for killing intracellular parasites and for perpetuating autoimmune responses. The Th2 response is associated with the promotion of IgE and eosinophilic responses in atopy, and is also associated with the production of interleukin-10, which has an anti-inflammatory response³. Excessive pro-inflammatory responses can lead to uncontrolled tissue damage, so excessive Th2 responses will counteract the Th1 mediated action.

Tumor immunology – The concept of immunoediting: elimination, equilibrium and escape

Normal cells in the body grow and divide in a controlled way in order to replace senescent or damaged cells. Sometimes, however this orderly process goes wrong. The genetic material of a cell can become damaged or changed, producing mutations that affect normal cell growth and division. When this happens, the cells grow uncontrolled, loose anoikis (the process by which the cell undergoes apoptosis after losing cell-to-cell interaction), and

adopt a migratory phenotype that is able to invade other tissues, giving rise to malignant neoplasms⁷.

The idea that the immune system surveys, recognizes and eliminates continuously arising tumor cells even in the absence of therapeutic intervention has gained widespread acceptance in the 1990s with the demonstration of the importance of IFN- γ in promoting immunologically induced rejection of transplanted tumor cells, and with the demonstration that mice lacking either IFN- γ responsiveness or the RAG-2 gene (mice that lack T, B and NK cells) were more susceptible to both chemically induced and spontaneous tumors⁸.

Indeed, the immune system detects the presence of dysregulated cells and developing tumors, destroying them before they become clinically apparent⁹. The liberation of pro-inflammatory cytokines, IFN- γ , damage-associated molecular pattern molecules (DAMPs) and stress ligands¹⁰ stimulates the innate immune response, while tumor antigens propagate the expansion of effector T cells⁹. The main protection against malignant cells is achieved via T-lymphocytes. Within T-lymphocytes, the glycoprotein CD3 is the cellular part responsible for recognizing processed antigens¹¹, such as those expressed by tumor cells. These antigens cause the differentiation of naïve CD4+ T cells into Th1 cells that produce IFN- γ , which in turn promotes CD8 T cell-mediated adaptive immunity¹². If successful, tumor destruction goes to completion, reaching an endpoint.

On the other hand, if a cell variant is not destroyed, it enters an equilibrium phase where the tumor phenotype populates a niche in which the immune system fails to exert its full strength. Eventually, this process leads to

an imperfect eradication of tumor cells and tumor progression by exerting a potent selection pressure on the heterogeneous and genetic unstable tumor cells. This selection of tumor cells that are fitter to survive in an immunocompetent host, a process termed immunoediting, results in cell variants that are no longer recognized and fought by the immune system, because of antigen loss or defects in antigen processing and presentation¹³. This problem bears resemblance to microbiology, where insufficient killing of pathogens may lead to the emergence of more resistant strains.

In the final escape phase, tumor cells that have acquired the ability to circumvent immune recognition emerge and become clinically detectable¹⁴. Loss of tumor antigen expression is one of the best studied-escape mechanisms¹³. Discovered more recently, a second mechanism appears to be a crucial component of tumor escape and apparently results from the establishment of an immunosuppressive state within the tumor microenvironment¹⁵. Tumor cells can impede the development of an anti-tumor response through the elaboration of cytokines such as VEGF, TGF- β or IDO and by recruiting regulatory T cells with immunosuppressive activity^{15,16}.

In humans, the evidence of immune changes in the tumor microenvironment comes from data showing that tumors contain higher levels of Treg and T lymphocytes than healthy tissue¹⁶⁻¹⁸. Essentially, all tumors contain significantly higher amounts of Treg and T-lymphocytes than adjacent normal tissue, such as individuals with lung or ovarian cancer¹⁹ and breast or pancreatic cancer²⁰. Furthermore, a number of reports on melanoma²¹, ovarian cancer¹⁷ and colon cancer²² patients demonstrate a correlation between tumor-infiltrating lymphocytes and patient survival.

Immune-privileged (IP) and non-immune privileged (NIP) sites

The vast majority of human organs are under efficient immunological surveillance and are thus regarded as non-immune privileged (NIP). However, in certain tissues or organs of the body, including brain, eyes, testis and the ovaries, the presence and induction of foreign antigens do not elicit a standard immunological response. These sites are considered immune-privileged (IP). Such immune privilege is exhibited by physical lack of lymphatic drainage, downregulation of MHC molecules, constitutive expression of Fas ligand or the local production of immune suppressive cytokines²³. Considered a key component of immunological tolerance, Treg have been proposed to maintain immune privilege in the eye and in the central nervous system, but other groups suggest that there is no contribution by Treg to achieving immune privilege in immune privileged organs¹⁴.

Regulatory T cells and their phenotypic markers – The transcription factor FOXP3

As described in the previous chapter, Tregs play a major role in cancer-induced immunosuppression, often negatively correlating with survival. These cells are a specialized subpopulation of T cells that act to suppress the activation and expansion of cells from adaptive and innate immunity, thereby hampering immune responses. In cancer patients, dendritic cells may be involved in the peripheral generation of Treg because dendritic cells, when exposed to tumor cells, acquire an immunosuppressive phenotype associated

with the induction of Tregs²⁴. These tumor-induced Tregs are phenotypically indistinguishable from other Tregs^{25,26}.

The identification and quantification of Treg cells changed as advances in the discovery of phenotypic markers were made that allow a more accurate and reliable quantification. Formerly the CD25 molecule, the α -chain of the IL-2 receptor, was the first candidate for a phenotypic definition of suppressive cells²⁷. Treg are vitally dependent on external IL-2 and therefore constitutively express the IL-2R²⁸. Although CD25 was sufficient to characterize and further analyze a relatively homogeneous population of Treg in mice living under pathogen-free conditions, this alternative is not possible in humans, who are continuously exposed to immunogenic stimuli resulting in T cell activation, IL-2 production and consequently CD25 upregulation²⁹. As an effort to circumvent the problem, the phenotype of human Treg was narrowed to CD25^{high} T cells³⁰. After the discovery that the FOXP3 gene^{31,32} encodes a transcription factor acting as a master regulator of Treg development and function^{33,34}, it was established as a new marker. Major concerns arose when it became evident that FOXP3 expression could be transiently induced in CD4⁺ and CD8⁺ effector cells upon stimulation³⁵ and when it was detected at low levels in CD25⁺CD4⁺ T cells³⁴. The human FOXP3 gene is located on the Xp11.23 and contains 11 coding exons. Exon-intron boundaries are identical across the coding regions of the mouse and human genes³⁶. While the precise control mechanism has not yet been established, FOX proteins belong to the forkhead/winged-helix family of transcriptional regulators and are presumed to exert control via similar DNA binding interactions during transcription. FOXP3 encodes a transcription factor called Scurfin that is

thought to dimerize with the nuclear factor of activated T cells, leading to suppression of IL-2, IL-4 and IFN- γ and inducing CD25, CTLA-4 and GITR³⁷.

More recently, Baron et. al suggested that a major criterion for the lineage commitment of Treg is the sustained expression of FOXP3 achieved by DNA methylation, as compared to the transient expression found in FOXP3 effector cells³⁸. A specific methylation pattern, specifically a demethylated DNA sequence within the FOXP3 locus associated with stable FOXP3 expression, was identified as a Treg specific demethylated region³⁸, making demethylated FOXP3 the most reliable Treg marker discovered to date.

Epigenetics and DNA Methylation

As previously described, the major criterion for lineage commitment of Treg is the epigenetic change of the FOXP3 gene. Epigenetics refers to heritable changes in gene expression other than the DNA sequence itself, but which do not involve modification of the underlying DNA sequence. An example of such changes is DNA methylation, which serves to suppress gene expression without altering the sequence of the silenced genes. Indeed, methylation of the 5'-carbon of cytosine residues in CpG sequences of DNA has long been recognized as an epigenetic silencing mechanism of fundamental importance, being maintained by a number of DNA methyltransferases, and having fundamental roles in the silencing of transposons and defense against viral sequences³⁹. The enzyme involved in this process is DNA methyltransferase, which catalyzes the transfer of a methyl group from S-adenosyl-methionine to cytosine residues to form 5-methylcytosine, a modified base that is found mostly at CpG sites in the

genome⁴⁰. CpG sites ("—C—phosphate—G—") are regions of DNA where a cytosine nucleotide occurs next to a guanine nucleotide in the linear sequence of bases along its length. They are usually clustered in CpG islands located near approximately 60% of promoters of genes and are usually methylation free, in order to actively transcribe the genes under their command⁴¹. The presence of methylated CpG islands in the promoter region of genes can suppress their expression. This process may be due to the presence of 5-methylcytosine that apparently interferes with the binding of transcription factors or other DNA-binding proteins to block transcription⁴⁰.

Epigenetic changes caused by DNA methylation can be used to differentiate and quantify cell populations. The intergenic region of the CD3 gene allows the identification of overall T lymphocytes because the CpGs of the CD3 region remain demethylated both in CD4+ (including Treg) and CD8+ T-lymphocytes, whereas granulocytes, monocytes, B-lymphocytes and NK-cells present a methylated CD3 pattern¹⁶. Through bisulfite conversion of genomic DNA, unmethylated CpGs are converted to TpGs, whereas methylated CpGs remain as CpGs residues, allowing the discrimination between both variants. Bisulfite conversion of CpG dinucleotides in the intergenic region of the CD3 gene allows the identification of overall T lymphocytes because the CpGs of the CD3 region are completely converted to TpGs (hence the CD3 gene remains demethylated) in CD4+ (including Treg) and CD8+ T-lymphocytes, whereas bisulfite-conversion in granulocytes, monocytes, B-lymphocytes and NK-cells results in the CpG-variant only¹⁶. In the case of Treg the demethylation at a highly conserved region within the human FOXP3 gene, called Treg-specific demethylated region (TSDR), FOXP3 locus is restricted to Treg cells, thus serving as the currently most

specific marker for the identification of cells with stable Treg phenotype and function (Fig. 1)³⁸. Hence, the CpGs of the FOXP3 gene are completely converted to TpGs by bisulfite-conversion, whereas bisulfite conversion of granulocytes, monocytes, naïve B cells, naïve T cells and all memory cell populations as well as several other tissues³⁸ results in the CpG-variant only. After bisulfite conversion, the use of quantitative real-time PCR assays (qPCR) for FOXP3 allows the specific and sensitive determination of Treg numbers by measuring demethylated FOXP3 TSDR DNA (Fig. 2)⁴².

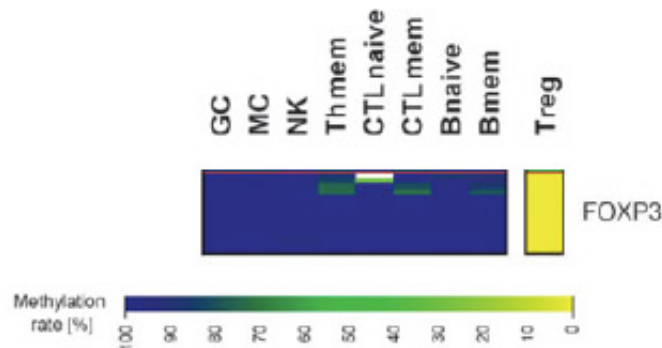


Figure 1 - Analysis of FOXP3 as a Treg-specific methylation marker in blood cell subtypes and non-hematopoietic tissues. DNA methylation pattern of FOXP3 was analyzed in indicated leukocyte subtypes sorted from pooled peripheral blood of healthy donors. The DNA methylation patterns of 12 differential methylation hybridization (DMH)-derived candidate genes were also analyzed (data not shown). Adapted from³⁸.

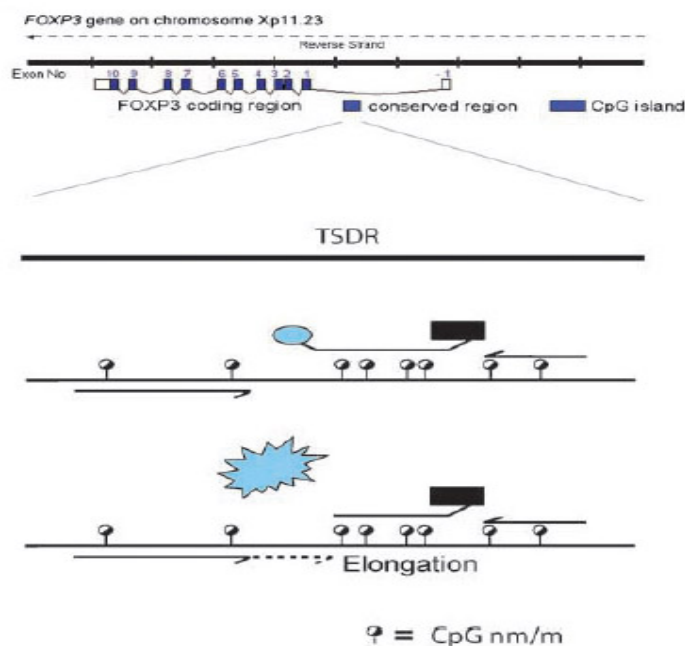


Figure 2 – A schematic overview of the FOXP3 locus and the amplification strategy. Two methyl-sensitive amplification primers and methyl-sensitive hybridization probes are used. The detection dye, which is quenched, whereas the probe is intact, is released upon exonuclease digestion during specific strand elongation⁴².

Epithelial ovarian cancer and borderline ovarian tumors

Epidemiology, risk Factors, pathogenesis and screening

Epithelial ovarian carcinomas (EOC) account in 90% of malignant ovarian tumors⁴³. Approximately 8,000 new cases are diagnosed annually in Germany, of which approximately 75% are at an advanced stage⁴⁴. BOT account for 10 to 20% of ovarian epithelial tumors, of which more than 80% are stage I⁴⁵.

Whereas at present it is unclear which factors play a role in the different paths of these disease entities, it is known that BRCA gene mutations account for 10 to 15% of all EOC⁴⁶. However, neither these mutations nor a positive family history appears to increase the risk for BOT^{47,48}. The theory of incessant ovulation states that the epithelial surface of the ovary is ruptured regularly at ovulation and then repaired by cell division, introducing the potential for cell mutations⁴⁹. Therefore factors affecting ovulation, such as nulliparity, early menarche, late menopause⁴⁹ and a lifelong irregular menstrual pattern⁵⁰ are known risk factors for developing EOC, whereas the prolonged use of the oral contraceptive (OC) pill reduces the risk, this protective effect persisting after cessation of OC usage⁵¹. In contrast, oral contraception does not appear to be protective for BOT. The use of fertility drugs was reported as a risk factor for development of BOT in some studies, although other studies have not shown this association^{50,52}. Whether there is a link between infertility drugs and EOC is equally controversial, although most recent studies suggest no link between the treatment itself and EOC⁵². There is arguable evidence that some environmental factors may also play a

role, namely talcum powder^{53,54}, cigarette smoking⁵⁵, diet⁵⁶⁻⁵⁹, exercise^{60,61} and obesity⁶².

EOC derives from malignant transformation of the epithelium of the ovarian surface, which is contiguous with the peritoneal mesothelium. One of the main challenges of EOC and BOT is the current lack of a progression model for these diseases. For many years, BOT was considered to be a pre-malignant disease. However, based on a review of molecular and clinicopathological studies, two main pathways of tumorigenesis have been proposed. Type I tumors include low-grade G1 neoplasms that arise in a stepwise fashion from a cystadenoma or a borderline tumor, whereas type II tumors are high-grade G2/3 neoplasms for which precursor lesions have not been identified, so-called *de novo* development⁶³⁻⁶⁵. Among the most studied molecular alterations are the mutations in KRAS and BRAF oncogenes in low-grade carcinomas and mutations in the *p53* gene in high-grade carcinomas⁶⁶. Mutations in either KRAS or BRAF were reported to occur in low-grade invasive micropapillary serous carcinomas and serous borderline tumors. In contrast, none of the conventional aggressive high-grade serous carcinomas contains BRAF or KRAS mutations, suggesting that low grade and high-grade ovarian carcinomas develop through independent pathways (Fig. 3, Table 1)⁶⁶. These findings however seem to be challenged by the most recent findings of the ROBOT study where 7.8% of the BOT patients relapsed, 30% of them with invasive EOC. Of these, 36% were shown to be high-grade EOC⁴⁵.

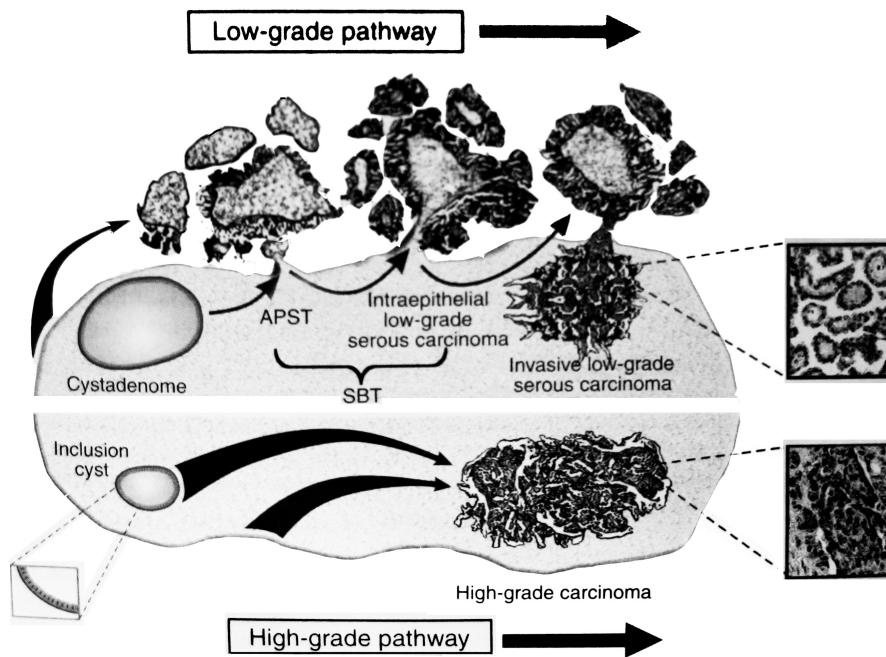


Figure 3 – Schematic representation of the dualistic model of development of ovarian serous carcinomas, the most common type of ovarian cancer. APST – Atypical Proliferative Serous Tumor; SBT – Serous Borderline Tumor (adapted from ⁶³)

Risk (R) / Protective (P) Factors	EOC	BOT
BRCA mutations (R)	Yes ⁴⁶	No ^{47,48}
Menstrual History (R/P)	Yes ⁴⁹	No ⁴⁹
Contraceptive Pill (P)	Yes ⁵¹	No ⁵¹
Fertility Drugs (R)	No ⁵²	? ^{50,52}
BRAF / KRAS mutations (R)	No ⁶⁶	Yes ⁶⁶
p53 mutations (R)	Yes ⁶⁶	No ⁶⁶
HER2 amplification (R)	Yes ⁶⁶	No ⁶⁶

Table 1 – Known risk or protective factors for EOC and BOT.

Diagnosis and histopathology

At present, there isn't any sensitive and specific tool to screen for EOC or BOT in the general population⁶⁷. The first results from a study of a new two-stage diagnostic approach, including post-menopausal women at average risk, using the CA-125 blood-test and an algorithm called ROCA (Risk of Ovarian Cancer Algorithm), showed promising results with very few false-positives and 99.9% specificity⁶⁸. Ultrasound examination is the most useful non-invasive diagnostic test in women with an adnexal mass, with pattern recognition by an experienced professional identifying up to 93% of the tumours as benign or malignant⁶⁹. The CA-125 is an antigen (a glycoprotein encoded by the MUC16 gene, secreted into the blood) that is elevated in about 80% of epithelial ovarian cancer patients. However, it only returns a true positive result for about 50% of Stage I ovarian cancer patients, and has a high frequency of false positive results, particularly in pre-menopausal women^{70, 71}. Because detecting early disease is the goal of screening, CA-125 is not an adequate screening test. According to ACOG/SGO guidelines, women with an elevation on the CA-125 (>35 U/L if postmenopausal, >200 U/L if premenopausal), ascites, evidence of abdominal/distant metastasis or family history of breast or ovarian cancer (in a first degree relative) should be referred to a gynaecological oncologist⁷².

Besides ovarian epithelial ovarian cancer (cystadenocarcinoma), the classification by the International Federation of Gynecology and Obstetrics (FIGO) subdivides other tumorous conditions associated with uncontrolled growth of ovarian epithelium according to their cellular behavior into benign

cystadenoma and cystadenoma with proliferating activity of the epithelial cells and nuclear abnormalities, but with no infiltrative destructive growth (also known as borderline ovarian tumors)⁷³. This is a cellular classification and therefore the differential diagnosis is achieved only histologically, with prognosis and clinical behavior varying considerably between these three conditions. Benign cystadenoma are composed of simple, non-stratified epithelium, with no cytologic atypia, while BOTs are cystadenomas characterized by proliferating activity of epithelial cells and variable nuclear atypia, but with no stromal invasion.

Papillary serous histology accounts for as many as 75% of EOC cases⁷⁴. Although no universal grading scheme exists for ovarian serous carcinoma, a two-tiered system (low-grade versus high-grade) has received increasing acceptance⁷⁴. Histopathologic grade is of prognostic significance and may also be of predictive value in that low-grade tumors appear less aggressive but also less chemotherapy responsive than high-grade tumors^{75,76}.

The absence of stromal invasion defines BOT⁷⁷. Isolated foci of microinvasion are found in approximately 5-10% of borderline serous tumors^{45,78}.

The term “serous borderline tumor with stromal microinvasion” rather than invasive carcinoma is appropriate when the invasive lesions do not exceed 3 mm in maximum dimension and the area does not exceed 10mm²⁷⁹. Serous tumors have a disproportionately high frequency of extraovarian disease with peritoneal implants being found at initial diagnosis in approximately 20% of patients, compared to 3% in mucinous BOT⁴⁵. On the other hand, virtually all mucinous borderline tumors are Stage I and have an

excellent prognosis, with 98% survival at 10 years, most treated solely by unilateral salpingo-oophorectomy⁸⁰, while approximately 25% of serous BOT are diagnosed at stage II/III⁴⁵. Peritoneal implants are classified as invasive or non-invasive. Invasive implants are found in 0.7% to 3.4% of cases and are commonly found together with noninvasive implants⁴⁵. Invasive growth and severe cytologic atypia correlate with an adverse prognosis⁸¹. While the corrected survival for patients with disease confined to the ovary is 100% at 15 years⁸², more than 30% of patients with ovarian serous borderline tumors with invasive implants will develop persistent or recurrent tumor, most commonly low grade serous carcinoma⁸³. For the group of patients with invasive implants, there is no consensus regarding standard therapy, although most oncologists will agree on the need for adjunctive chemotherapy.

Surgical staging and adjuvant treatment

EOC metastasizes almost exclusively via the transcoelomic route with about 70% of patients having peritoneal metastases at primary diagnosis⁷. Haematogenous metastases, involving distant organs such as the brain or bone, are very rare at primary diagnosis (PD)⁷. Ovarian malignancies are surgically staged according to the 2002 revised American Joint Committee on Cancer (AJCC) and International Federation of Gynecology and Obstetrics (FIGO) joint staging system⁸⁴. Some oncologists stage BOT using the same FIGO criteria as for other ovarian tumors, while others would stage them only according to presence and type of implants⁴⁵. The distribution of EOC and BOT worldwide by stage at presentation is presented in Table 2.

Stage	Tumor Spread	EOC	BOT
I	Disease confined to the ovaries	23 – 33%	70%
II	Disease extended into the pelvis	19 – 13%	10%
III	Disease extended to the peritoneal cavity outside the pelvis	46 – 47%	19%
IV	Distant Metastasis	12 – 16%	< 1%

Table 2 – Worldwide relative distribution of EOC according to stage at presentation^{85, 86}.

In the setting of EOC, the tumor should be resected and the histologic diagnosis confirmed. Consultation with a gynecologic oncologist experienced in ovarian cancer surgery is crucial^{87,388}. A total hysterectomy with bilateral salpingo-oophorectomy (TAH-BSO) should be performed (if the contralateral ovary appears normal, a unilateral salpingo-oophorectomy may be considered for apparent stage IA in women who strongly desire to preserve fertility. Contralateral ovarian biopsies are contraindicated because clinically occult bilateral ovarian involvement has been noted in only 2.5% of women undergoing staging for ovarian malignancy and ovarian surgery may impair future fertility, culminating in mechanical infertility in up to 14% of the cases⁸⁹). In case of stages I or II, as well as III or IV with clinical or radiological positive lymph nodes, bilateral systematic pelvic and para-aortic lymphadenectomy up to the left renal vein level should be performed. There are no clinical trials available in the case of clinical or radiological negative lymph nodes, although current retrospective data tend to favor lymphadenectomy^{90,91}. The currently ongoing LION trial (Lymphadenectomy In Ovarian Neoplasms) should address this issue in the near future.

The need for complete surgical staging of BOT is controversial. While some studies show no major differences in recurrence and survival rates

between the unstaged and staged patients⁹²⁻⁹⁶, the recent ROBOT study reported staging quality as a prognostic factor. Incomplete staging showed an elevated risk of recurrence compared to comprehensive staging (HR 1.77; 95% CI 1.15–2.71; p=0.0091) and re-staging after initial surgery had a beneficial impact with respect to PFS (HR 0.577; 95% CI 0.36 – 0.92; p=0.0214)⁴⁵. Lymphadenectomy is not performed in BOT because a 98% survival at 6.5 years is found in women with lymph node involvement⁹⁷. TAH-BSO is recommended for women beyond the fertile years or with advanced disease⁹⁸. The advantages of staging are to provide better information for prognostic counseling, to discover areas of occult invasion, and to obtain information about the biological behavior of these tumors. For these reasons, most oncologists recommend a comprehensive staging procedure for all patients, although others would disagree.

For the purpose of adjuvant treatment, anything other than Stage I EOC represents advanced disease and there is consensus on the following chemotherapeutic recommendations for this group of patients. The combination of cisplatin + paclitaxel proved superior to cisplatin + cyclophosphamide, the previous gold standard. Based upon the favorable safety profile of carboplatin plus paclitaxel and the survival benefits demonstrated in both GOG 111 and OV-10 studies^{99,100}, the current standard of care for debulked epithelial ovarian cancer is six cycles of carboplatin plus paclitaxel. For women with advanced disease, response rates approach 90%, with 75% achieving a clinically complete response¹⁰¹. However, up to three quarters of those with a complete clinical response relapse and require further treatment. On the other hand, in the setting of BOT most clinicians would

agree that there is no advantage for chemotherapy in women with early stage, optimally cytoreduced disease. Its use for women with invasive implants is however controversial. Many clinicians believe that the presence of invasive peritoneal implants is associated with a poorer prognosis and should exclude its categorization as a tumor of low malignant potential. These patients are at higher risk of persistent/recurrent disease and may be considered for chemotherapy.

Of note, for women presenting with early stage EOC, the following recommendations are made¹⁰²:

- Patients with stage IA or IB grade I tumors do not require adjuvant therapy
- All patients with grade III tumors require adjuvant treatment
- All patients with clear cell carcinoma require adjuvant treatment
- Consensus on the need for adjuvant treatment in the remaining subsets of patients with stage I disease could not be reached

Aim

Is there a correlation between different cellular ratios of immune tolerance in the tumor microenvironment and the clinical outcome in borderline ovarian tumors and epithelial ovarian cancers?

Is there a correlation between peripheral changes in the cellular ratios of immune tolerance and the transcoelomic metastatic pattern in epithelial ovarian cancer?

BOT and EOC are two forms of ovarian malignancy with very different clinical courses and treatment approaches. These tumors spread almost exclusively via the transcoelomic route, whereas haematogenous metastases are seldom present at primary diagnosis⁷. BOT generally follows a benign course, whereas survival is generally poor in women with EOC — in part secondary to stage distribution. Despite the excellent prognosis, some patients — particularly those with invasive implants — eventually recur with BOT. Approximately 30% of the BOT patients suffering a recurrence may develop high-grade carcinoma⁴⁵. Therefore BOTs are one of the most controversial topics in gynecologic oncology and pathology, and are confusing to both clinicians and patients. Although these tumors are considered to be a subset of malignancy, most patients are cured when the disease has been adequately treated⁸². Unfortunately, the category has also led to a clinical dilemma because many patients with BOT are young and wish to preserve their fertility. Because BOT are regarded as malignant, their treatment has often been more aggressive than is necessary based on their behavior, which is generally benign. This difference in aggressiveness poses a clinical problem because there are no cellular or molecular markers capable of predicting this difference in outcome. Current data supports the hypothesis

that Treg play an important role in disrupting the immune response to cancer cells, appearing to play a pivotal role in the avoidance of immune surveillance¹⁶⁻¹⁸. We postulate that a central difference between the tumor-entity specific behaviors, including the particular transcoelomic dissemination pattern, is the ability of the immune system to counteract these diseases.

The main purpose of this work is to examine whether changes in the Cellular Ratio of Immune Tolerance, a concept here introduced for the first time – immunoCRIT - are tumor-type-dependent and therefore a potential cause for the differential disease outcome and hence a marker for disease aggressiveness. ImmunoCRIT, as the name indicates, refers to the ratio of Treg in the overall T lymphocytes, determining the level of Treg-mediated immunological tolerance, while excluding the vascularization-associated factor.

Secondarily, it is proposed that normal levels of immunoCRIT in the peripheral blood of patients with disease confined to the abdomen prevent tumor cells from spreading by the hematogenous route. This could provide evidence for the relevance of Treg FOXP3+ cells in the development and counteraction of these tumors and their aggressiveness as well as an explanation for the tumour dissemination pattern.

In order to test our hypothesis the number of overall and regulatory T cells in tumor tissue and in peripheral blood will be quantified. To exclude an increase in the number of immune cells due to an increase in tumor perfusion, we will further assess the ratio of regulatory T cells relative to the percentage of overall lymphocytes, here referred to as immunoCRIT. We have a large

cohort of IP and NIP samples, namely breast, colorectal, kidney and lung cancer (NIP) and cystadenoma, BOT (both invasive and non-invasive) and EOC (both early and late stage) (IP).

Primary question

- Does the tissue immunoCRIT differ between IP and NIP sites, and within NIP sites does it differ between non-invasive-, invasive-BOT and LSOC?

Secondary questions

- Do the levels of peripheral immunoCRIT differ in patients with distant metastasis that require the hematogenous route?
- Does this difference reflect the immune privilege status (IP vs. NIP)?

Materials and Methods

Tissue samples, patient and data collection

The epithelial ovarian cancer samples were obtained from the OVCAD (Ovarian Cancer Diagnosis Initiative) study and from the European Center for Ovarian Cancer Tumor Bank, Charité Campus Virchow (Germany). In both cases patients with a histological diagnosis of primary epithelial ovarian cancer were enrolled and followed. Ovarian cancer patients having a second malignancy were excluded from this study. Tumor tissue samples were obtained from all patients prior to any chemotherapy treatment. The tumor tissue was placed immediately on ice after being removed from patients and processed within 20 minutes. It was cut into four pieces with approximate 2 x 50 mg, 1 x 100 mg, 1 x 200 mg in weight and these were cut into smaller pieces (approximately: 2 x 2 x 2 mm). Subsequently the samples were placed in four 1.8 ml Nunc Cryotube vials and stored in liquid nitrogen or -80°C upon delivery.

All patients were treated with first-line standard chemotherapy, 6 cycles of carboplatin (75 mg/m² over 30 minutes) plus paclitaxel (175 mg/m² over a three-hour period), if tolerated. Systematic follow-up was performed by all centers according to guidelines¹⁰³, clinical data were prospectively collected and documented using validated SOPs. The date of initial surgery was taken as the date of diagnosis. Surgical stage and histological grade and cell type were categorized according to International Federation of Gynecology and Obstetrics and World Health Organization standards. Each patient was

classified as a responder or non-responder to platinum-based chemotherapy. Patients were considered responders if they were platinum-sensitive (recurrence >6 months after the last cycle of platinum-based therapy) and non-responders if they were platinum-resistant (recurrence <6 months of platinum-based therapy). This classification was based on symptoms, physical examination and radiological exams. Progression-free survival was estimated as the time from initiation of primary therapy to the date of detection of recurrent disease. Duration of overall response was estimated from the time of response to the date of recurrence or disease progression. All relevant clinical data, including surgical documentation, were entered in an online data bank.

The borderline ovarian tumor samples and the peripheral blood samples were obtained from the European Center for Ovarian Cancer Tumor Bank, Charité Campus, Virchow (Germany), according to availability. All relevant clinical data, including surgical documentation, were prospectively collected, documented using validated SOPs and entered in the clinical tumor data bank. All the patients were surgically staged and none received adjuvant treatment. For the purpose of this study, data regarding age, presence and type of implants as well as recurrence and death were used.

The colorectal and bronchial samples were derived from a previous publication by our research group¹⁶. The mammary and renal samples were kindly provided by a post-graduate researcher working in the project and co-author of the publication derived from this work.

Histology

The histology was reviewed by Provitro GmbH (Berlin, Germany). All tissue samples with <50% tumor were excluded.

DNA Extraction

Tissue

Double-strand genomic DNA from tumor tissue was isolated using the DNeasy Tissue Kit to yield a final volume of 100 μ l. First, 180 μ l Buffer ATL was pipetted into a 2 ml microtube and approximately 10 mg of tissue was added to the tube. After homogenization and centrifugation, 20 μ l proteinase K was added to the tube. Incubation was performed overnight at 56°C. After centrifugation, 200 μ l of buffer AL was added to the sample and mixed thoroughly by vortexing. After that, 200 μ l ethanol (96%) was added and again mixed thoroughly by vortexing. The mixture was then pipetted into the DNeasy Mini spin column, placed into a 2 ml collection tube and centrifuged at $\geq 6,000 \times g$ (8000 rpm) for 1 min. The flow-through and collection tube were discarded. The DNeasy Mini spin column was then placed in a new 2 ml collection tube, 500 μ l Buffer AW1 was added and centrifuged for 1 min at $\geq 6,000 \times g$ (8000 rpm). Again, the flow-through and the collection tube were discarded. The DNeasy Mini spin column was put in a new 2 ml collection tube and 500 μ l of Bbuffer AW2 was added. Centrifugation for 3 min at 20,000 $\times g$ (14,000 rpm) to dry the DNeasy membrane followed. The flow-through and collection tube were discarded. The DNeasy Mini spin column was then

placed in a clean 2 ml microcentrifuge tube and 200 μ l of buffer AE was pipetted directly onto the DNeasy membrane. After incubation at room temperature for 1 min and centrifugation for 1 min at $\geq 6,000 \times g$ (8,000 rpm), elution with 100 μ l was performed. This last step was performed three times.

Blood

Double-strand genomic DNA from blood was isolated using the DNeasy Blood Kit to yield a final volume of 100 μ l. First 20 μ l proteinase K was pipetted into a 1.5 ml or 2 ml microcentrifuge tube and 5 to 10 μ l of anticoagulated blood was added. The volume was then adjusted to 220 μ l with PBS and 200 μ l of Buffer AL was added. The resulting mix was thoroughly vortexed, and incubated at 56°C for 10 min. Then 200 μ l ethanol (96%) were added to the sample, and mix thoroughly by vortexing. The mixture was pipetted into a DNeasy Mini spin column placed in a 2 ml collection tube and centrifuged 8000 rpm for 1 min. The flow-through and collection tube were discarded. The DNeasy Mini spin column was placed in a new 2 ml collection tube and 500 μ l of Buffer AW1 were added. After centrifuging for 1 min at 8000 rpm the flow-through and collection tube were discarded. The DNeasy Mini spin column was placed in a new 2 ml collection tube and 500 μ l Buffer AW2 were added. After centrifuging for 3 min at 14,000 rpm to dry the DNeasy membrane, the flow-through and collection tube were discarded. The DNeasy Mini spin column was placed in a clean 1.5 ml microcentrifuge tube and 200 μ l Buffer AE were pipetted directly onto the DNeasy membrane, followed by incubation at room temperature for 1 minute, and then centrifugation for 1 min 8000 rpm to elute. For maximum DNA yield, the elution was repeated once as described.

Sodium bisulfite conversion

During bisulfite conversion of genomic DNA, unmethylated CpGs are converted to TpGs, whereas methylated CpGs remain as CpGs residues, allowing the discrimination between both variants.

Sodium bisulphate treatment of genomic DNA was performed using the EpiTect Bisulfite Kit (Qiagen, Hilden, Germany) following the supplier's recommendations, using 500 ng of DNA to yield a final volume of 44 μ l. Bisulfite Mix aliquots were prepared by adding 800 μ l RNase-free water to each aliquot and vortexing until complete dissolution. Then, the bisulfite reactions were prepared in 200 μ l PCR tubes using a combined volume of DNA solution and RNase-free water of 40 μ l, 85 μ l of Bisulfite Mix and 15 μ l of DNA protect buffer.

The bisulfite DNA conversion was performed using a thermal cycler, with the following thermocycling conditions: 1 x 95 °C, 5 min; 1 x 60°C, 25 min; 1 x 95°C, 5 min; 1 x 60°C, 85 min; 1 x 95 °C, 5 min; 1 x 60°C, 175 min.

Once the bisulfite conversion was complete, after briefly centrifuging the PCR tubes containing the bisulfite reactions and transferring the complete bisulfite reactions to clean 1.5 ml microcentrifuge tubes, 560 μ l freshly prepared Buffer BL containing 10 μ g/ml carrier were added and the solutions were mixed by vortexing and then centrifugation. The entire mixture was transferred from the tubes into the corresponding EpiTect spin columns. After centrifuging the spin columns at maximum speed for 1 min, the flow-through was discarded and the spin columns were placed back into the collection tubes. Then, 500 μ l Buffer BW were added to each spin column and

centrifuged at maximum speed for 1 min, the flow-through was discarded and the spin columns were placed back into the collection tubes. Next, 500 μ l Buffer BD were added to each spin column and incubated for 15 min at room temperature (15–25°C). The spin columns were centrifuged at maximum speed for 1 min, the flow-through was discarded and the spin columns were placed back into the collection tubes. After adding 500 μ l of Buffer BW to each spin column and centrifuging at maximum speed for 1 min, the flow-through was discarded, the spin columns were placed back into the collection tubes and this step was repeated. The spin columns were placed into new 2 ml collection tubes and centrifuged at maximum speed for 1 min to remove any residual liquid. The spin columns were placed into clean 1.5 ml microcentrifuge tubes and 20 μ l Buffer EB was dispensed onto the center of each membrane. Finally, the purified DNA was eluted by centrifugation for 1 min at 15,000 x g (12,000 rpm).

PCR amplification

Real-time PCR was performed in a final reaction volume of 10 μ L using Roche LightCycler 480 Probes Master (Roche Diagnostics) containing 5 pmol each of non-methylation-specific and methylation-specific forward and reverse primers for FOXP3 and CD3, respectively, methylation specific hydrolysis probe (MWG) in a concentration of 5 pmol/ μ l, lambda DNA (New England Biolabs) in a concentration of 50 ng/ μ l and bisulfite-treated genomic DNA in a concentration of 500 ng/ μ l template and a serial dilution of plasmid standard ranging from 6250 to 10 plasmid units. Each sample was analyzed in triplicate

using a LightCycler 480 System (Roche). Cycling conditions consisted of a 1x (95°C 10 min), 50x (95°C 15 s, 61°C 1 min). The absolute quantification of copy number and the second derivative method algorithms were used for quantification.

Oligonucleotides forward (fp), reverse primers (rp) and probes (p) are indicated by chromosomal positions of human genome assembly GRCh37. The oligonucleotids used were CpG-specific FOXP3 (ENSG00000049768): fp:X:49117219-46:1, rp:X:49117283-307:1, p:X:49117256-3:1; TpG-specific: fp:X:49117219-46:1, rp:X:49117283-307:1, p:X:49117256-78:1 (b) CD3: CpG-specific: fp:11:118213633-53:1, rp:11:118213686-707:1, p:11:118213670-87:1; TpG-specific: fp:11:118213632-53:1, rp:11:118213686-709:1, p:11:118213664-90:1¹⁶.

Identifying cell populations

Experimentally we used quantitative QPCR of bisulfite converted DNA. For each region, we used one qPCR system that exclusively recognizes the TpG-template, and one that is specific for the CpG-template (Fig. 5 and 6) for FOXP3 or CD3. The CD3 assay determines the number of demethylated, and thus bisulfite converted accessible CD3 gene copies as an indicator of the number of CD3⁺ T-lymphocytes in relation to all CD3 gene copies as an indicator of the overall cell number in the analysed tissue specimen. The ratio of these counts corresponds to the relative number of T-lymphocytes amongst all nucleated cells in a given sample. The FOXP3 assay determines the number of bisulfite converted accessible FOXP3 gene copies as an indicator of the number of regulatory T-lymphocytes in relation to all FOXP3 gene

copies as an indicator for the overall cell number in the analysed tissue specimen.

In order to provide a copy number quantification standard, plasmid systems for both loci that correspond to TpG and CpG-variants were used. Using serial dilutions of plasmids containing the equivalent of bisulfite-converted TpG CpG DNA target regions as a standard, we determined DNA copy numbers. To provide a quantitative evaluation of tissue-infiltrating FOXP3+ Treg and overall CD3+ T-lymphocytes in solid tissues, we compared DNA isolated from borderline ovarian tumors and epithelial ovarian cancer tissue.

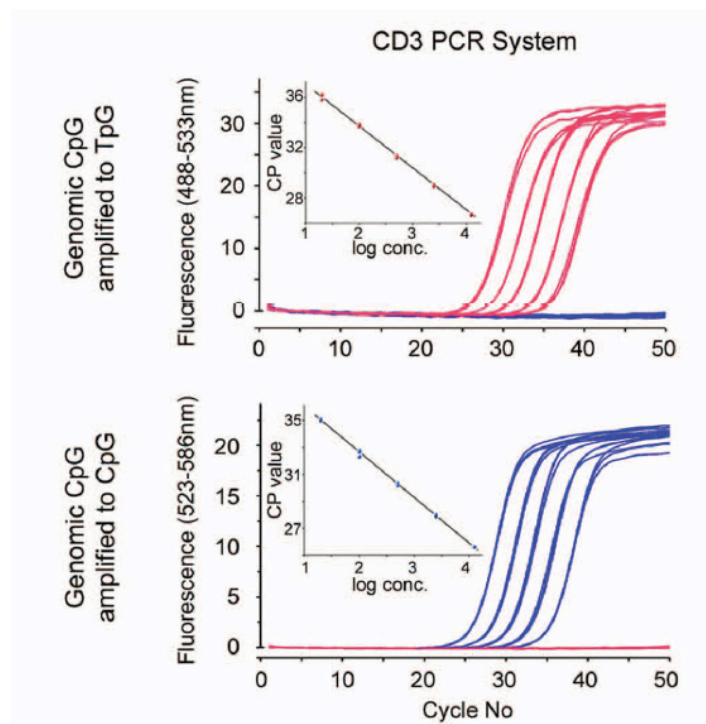


Figure 5 - Amplification profile of bisulfite-conversion specific qPCRs. Upper part: qPCR specific for TpG-variant tested on dilutions of 12,500, 2,500, 500, 100 and 20 plasmid copies representing TpG (red) and CpG template variants (blue). Lower parts: The same experiment using qPCR specific for the CpG-variant. Linearity of qPCRs is shown inside each graph by plotting CP-values over log-concentration of template¹⁶

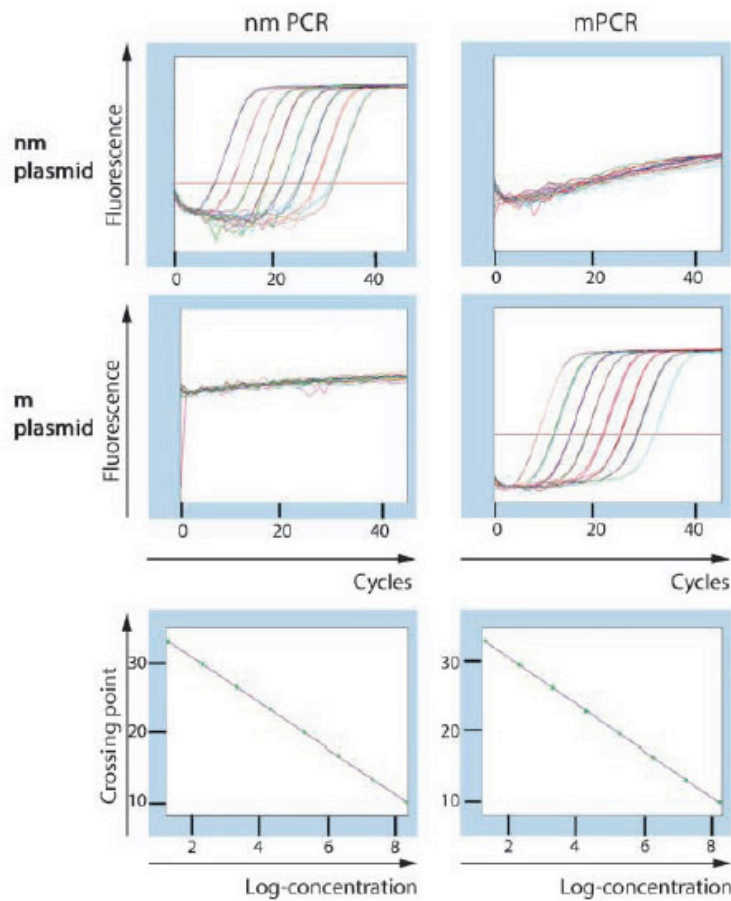


Figure 6 - qPCR system for the FOXP3 to detect Treg. Amplification profiles of the qPCR systems (top and middle). Left: nonmethylation-specific amplification system; right: methylation-specific amplification system. Top: a plasmid corresponding to nonmethylated (nm) FOXP3 is used in a serial dilution row ranging from 200 million to 20 copies. Middle, same dilution with a plasmid corresponding to methylated (m) FOXP3. Bottom: standard curves as produced by serial dilutions of plasmid present in a strictly log-linear fashion⁴².

The qPCR was carried out on dilutions of 12,500, 2,500, 500, 100 and 20 plasmid copies representing TpG and CpG template variants. The results obtained in the PCR assay consisted of clear sigmoid functions. By plotting the CP-values over the log-concentration of the template it was possible to obtain linearity. The absolute quantification of copy number and the second derivative method algorithms were used for quantification. The average copy number for the FOXP3 assay was 227.9 and 19640.3 for respectively TpG and CpG variants, respectively. For the CD3 locus these values were 1205.5 and 12127.4. These are realistic values and therefore allow further analysis.

Statistical analysis

Statistical analysis was performed with SPSS 16.0.

The means were compared for all of the categorical data measures. The Levene test for homogeneity of variance was used to determine whether the variances were similar. When the variances were similar, the analysis of variance (ANOVA) F test was used; when the variances were dissimilar, a robust test of equality of the means was used. Multiple comparison tests were used to determine which paired means were significantly different. Fisher's Least Significant Different Test (LSD) was used when the variances were not significantly different and the Tamhane test was used when the variances were different. A Bonferroni correction of $0.05/7=0.007$ was used for each of the continuous measures.

In addition to the overall chi-square test of the association between two variables, tests were also included to determine which pairs of column proportions differed. Fisher's exact test for two-by-two tables was used when expected values were small. For the chi-square test, a Bonferroni correction of $0.05/25=0.002$ was employed in order to avoid type I errors.

When the outcome of the variables was dichotomous, logistic regression was used. Forward and backward stepping was used. The odds ratio and $\exp(\beta)$ were determined with logistic regression.

We tested the significance of the observed trends by applying the Jonkheere-Terpstra test whenever there was one value per patient and by applying the Page trend test whenever there were different values (such as different disease time-points) for each patient.

Results

Characteristics of the cohort

Regarding the cohort of colorectal and bronchial cancer, please refer to our previous publication¹⁶. Regarding the mammary and renal cancer samples, these were provided by a post-graduate colleague from our laboratory.

Immune privileged - EOC

Of the 191 ovarian cancer tissue samples available for this study, 45 were excluded due to low percentages (<50%) of tumor, leaving a total of 146 samples. Early-stage (ESOC) patients were considered separately from late-stage (LSOC) patients because they present a different prognosis and in some cases even treatment approach.

The LSOC patients were followed for a mean of 24.7 ± 12.8 (1 - 49) months and are characterized in Table 2. Recurrence occurred in 62.9% patients and 48.4% died from the disease. Of the patients currently alive, 72.5% are alive with no evidence of disease and 27.5% are alive with disease. The cohort had a median progression-free survival (PFS) of 25.0 months (95% CI=18.97-26.20) and a survival rate at 2 years of 69.0%.

Characteristic	N (%)
Age (years)	57.5 ± 10.1 (33 – 85) years
Stage	
II	6 (4.1)
III	113 (77.4)
IV	27 (18.5)
Grade	
I	3 (2.1)
II/III	143 (97.9)
Histology	
Serous	122 (83.6)
Non-serous	24 (16.4)

Table 2 – Characteristics of patients with epithelial ovarian cancer

BOT

There were 50 samples of borderline ovarian tumors available for analysis. The characteristics of these patients are summarized in Table 3.

Characteristic	N (%)
Age (years)	48.8 ± 17.8 (15 – 87)
Invasive Implants	
Yes	12 (24.0)
No	38 (76.0)
Recurrences	
	12 (24.0)
Deaths	
	3 (6.0)

Table 3 – Characteristics of patients with borderline ovarian tumors

The mean duration of follow-up was 28.66 ± 32.09 months (1 – 98). Of note, the three deaths occurred in patients with invasive disease. Of the 12 patients with recurrent disease, 10 (83.3%) had invasive disease.

The small number of deaths (n=3) precludes survival analysis. The chi-square analysis showed that the presence of invasive implants significantly correlates with recurrence ($p < 0.0001$).

The use of a logistic regression model showed that the presence of invasive implants significantly correlated with recurrence, with an OR=17.0 ($p < 0.0001$). The model correctly predicted 84.0% of the recurrences.

Regarding the LSOC cohort, the relative distribution by histological type, survival rate and progression-free survival data are in accordance with the standard assumptions and previous results. In the BOT cohort the relative percentage of patients with invasive disease, as well as the percentage of deaths and recurrences are also in agreement with worldwide reported cohorts (see discussion). Hence our cohorts are representative of the population of EOC and BOT patients and therefore these cohorts are valid for further analysis as intended.

Tumor infiltrating lymphocytes

Overall T lymphocytes – CD3 marker

Analysis of tissue-infiltrating CD3-demethylated cells in tissues derived from non-immunoprivileged (NiP) vs. immune privileged (IP) organs

We analyzed the number of tissue-infiltrating T lymphocytes in solid benign and malignant tumorous tissue samples, applying the aforementioned epigenetic qPCR analysis. Overall, we used this approach on 273 benign samples and 589 malignant solid tissue samples originating from colorectum, kidney, lung, breast and ovary as well as on 50 borderline ovarian tumor tissues. The mean percentage of overall T lymphocytes (oTL) is described in Table 4.

	Non-immune Privileged Tissue			
	Benign	Malignant		
T-cells				
N	258	401		
Median (%)	31.86	21.64		
Immune Privileged Ovarian Tissue				
	Benign cyst	BOT	ESOC	LSOC
T-cells				
N	15	50	42	146
Median (%)	3.92	3.51	4.27	7.26

Table 4 – Median percentage of overall T lymphocytes in NIP and IP Tissues

As presented in Table 4 and in Figure 6, the median percentage of overall T cells (oTL) in 258 benign NIP tissues was 31.9%. The oTL counts in samples derived from benign IP ovarian tissue ranged between 4% and 7% and thus remained significantly lower ($p < 0.0001$) than in benign NIP tissues, while the median percentage in malignant NIP tissues, including colorectal, bronchial and mammary tissues, was 21.6%. This difference was shown to be statistically significant when including all NIP tissues ($p < 0.0001$), showing that the cellular T cell density in malignant NIP tissues was significantly lower than in healthy NIP tissues.

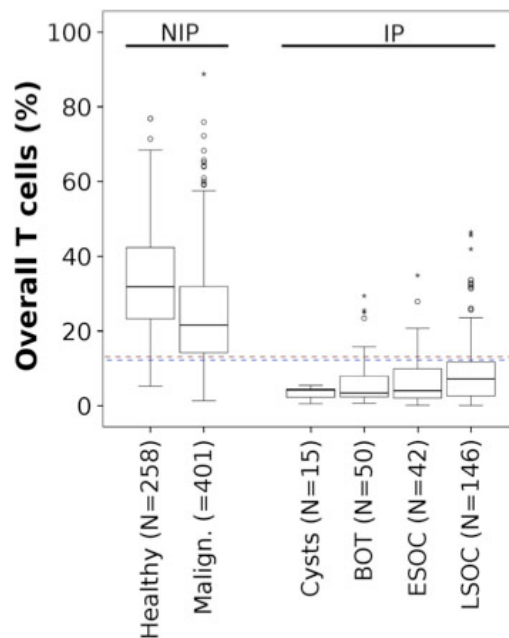


Figure 6 -. Frequency of T lymphocytes in tissue from healthy donors and patients with solid tumors as measured by the epigenetic CD3+ demethylation assay, frequency of infiltrating T lymphocytes in non-immune privileged (NIP) healthy and malignant (Malign.) tissues and several tissue types of immune privileged (IP) ovarian tissue (cysts, borderline ovarian tumor (BOT), early stage (ESOC) and late stage ovarian carcinoma (LSOC). N indicates the number of donors/patients in each plot. Boxes depict the middle 50% of the distribution, the line within represents the median. Whiskers extend to include 95% of all data, mild outliers are indicated by circles, extreme outliers by stars. Dotted lines represent the calculated cut-off values for most accurate segregation between healthy (green) and malignant NIP and IP tissues.

In order to determine whether this immunological privilege is maintained in cancer, 401 malignant NIP tissue samples including colorectal, breast and bronchial tissues as well as 146 malignant IP LSOC samples were compared. The oTL were shown to be lower in both benign and malignant tissue in IP tissues (both $p < 0.0001$). The main difference between IP and NIP resides in the finding that in IP tissues oTL levels are higher in malignant states ($p < 0.0001$) and in NIP tissues these levels are lower in malignant disease ($p < 0.0001$, Figure 6).

We still observed immunological differences between NIP and IP tissues, which however were less pronounced than in the benign tissues. We tested the significance of the observed trend that T cell infiltration experiences a gradual increase along with an increase in stage and aggressiveness of the disease by applying the Jonkheere-Terpstra test ($p = 0.003$). This test shows that BOT and ESOC have a more intact immunological status than LSOC. We conclude that both NIP and IP tissues remain immunologically largely intact and strictly segregated from each other, despite a detectable disruption of their immune status that goes along with malignant transformation.

Sub-analysis of the malignant IP tissues - BOT and LSOC

The median percentage of overall T lymphocytes (oTL) was 3.51% for BOT, 4.27% for ESOC and 7.26% for LSOC, this difference being statistically significant ($p = 0.001$). Regarding the patients without invasive implants ($n = 38$) the oTL levels were 3.02%, resembling the levels seen in benign cysts (3.90%), while the patients with invasive implants ($n = 12$) showed median oTL

levels of 8.78%, resembling the levels shown in LSOC (Fig. 7, Table 4). The difference between BOT with and without invasive implants is significant ($p=0.028$), as is the difference between BOT without invasive implants and LSOC ($p=0.001$). As expected, BOT with invasive implants does not differ from LSOC.

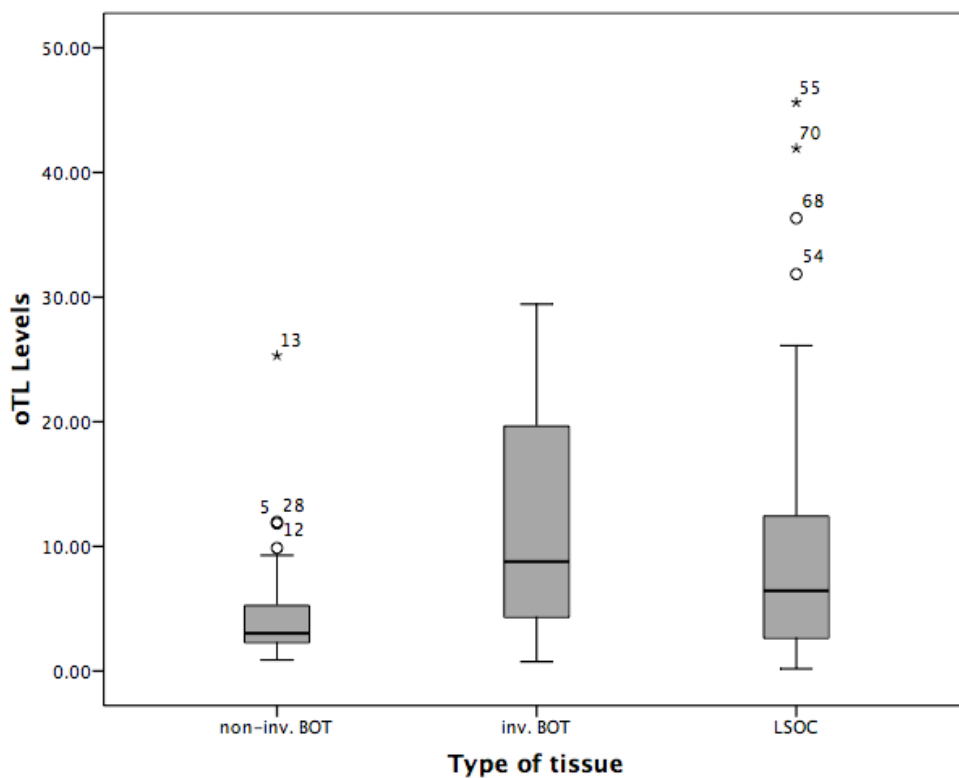


Figure 7 - Boxplot showing the percentages of CD3+ T cells in BOT without invasive implants (non-inv. BOT), BOT with invasive implants (inv. BOT) and LSOC. Boxes depict the middle 50% of the distribution, the line within represents the median. Whiskers extend to include 95% of all data, mild outliers are indicated by circles, extreme outliers by stars.

Tissue	Cystadenoma	Non-inv. BOT	Inv. BOT	LSOC
oTL Levels	3.90%	3.02%	8.78%	7,26%

Table 5 – Median oTL levels in the different tumorous conditions of the ovary, benign cystadenoma, BOT without invasive implants (non-inv. BOT), BOT with invasive implants (inv. BOT) and late stage ovarian cancer (LSOC)

In lung and colorectal cancers, oTL levels are shown to be reduced in comparison to their benign counterparts (Table 6). Bronchial cancer shows levels of 22.3% oTL and colorectal cancer shows levels of 26.1% oTL, while healthy tissue shows 29.6% oTL and 33.5% oTL, respectively. Our study shows that instead, LSOC presents double the levels of oTLs shown in healthy ovarian tissue, with infiltration of overall T-lymphocytes increasing from ESOC (4.3%) to LSOC (7.3%) (Table 6).

Tissue	Benign Cystadenoma			Bronchial	Colorectal
oTL Levels	3.90%			29.6%	33.5%
Tumorous Tissue	Non-inv. BOT	Inv. BOT	LSOC	Bronchial Cancer	Colorectal Cancer
oTL Levels	3.02%	8.78%	7.26%	22.3%	26.1%

Table 6 – Median oTL levels in the different healthy and tumorous tissues, the first group belonging to IP tissues, and the second to NIP tissues. Non-inv. BOT: BOT without invasive implants, inv. BOT: BOT with invasive implants, LSOC: late stage ovarian cancer

Epigenetic analysis of immunoCRIT in NIP and IP tissues

Regulatory T cells and immunoCRIT: Ratio of regulatory T cells relative to the percentage of overall T lymphocytes

We applied an epigenetic Treg assay, which determines the number of bisulfite conversion accessible FOXP3 gene copies, as an indicator for the number of regulatory T-lymphocytes in the aforementioned tissue specimens. The Treg values obtained were used to measure the ratio of Tregs to all T cells, in order to determine the level of Treg-mediated immunological tolerance, here referred to as immunoCRIT. The median Treg levels for the different benign and malignant IP and NIP tissues are shown in Table 7. We analyzed BOT without invasive implants separately from BOT with invasive implants and together with late stage ovarian cancer. The mean percentage of regulatory T cells was 2.18% (0.54% for non-invasive BOT, 1.36% for invasive BOT and 2.95 for LSOC) and it correlated with the histological diagnosis ($p < 0.0005$). Accordingly, the mean Treg level for the LSOC cohort is 2.95%, significantly higher than the average value for the invasive BOT cohort (1.36%, $p = 0.006$) and than the non-invasive BOT cohort (0.54%, $p < 0.0005$, Fig. 9, Table 7). The difference in immunoCRIT in benign cysts, BOT and LSOC show a significant difference, increasing progressively through the spectrum of these proliferative ovarian diseases ($p < 0.001$).

Tissue	Benign Cystadenoma			Bronchial	Colorectal
Treg Levels	0.12%			2.0%	1.9%
Tumorous Tissue	Non-inv. BOT	Inv. BOT	LSOC	Bronchial Cancer	Colorectal Cancer
Treg Levels	0.54%	1.36%	2.95%	4.2%	3.8%

Table 7 – Median Treg levels in the different healthy and tumorous conditions, the first group belonging to IP tissues, and the second to NP tissues. Non-inv. BOT: BOT without invasive implants, inv. BOT: BOT with invasive implants, LSOC: late stage ovarian cancer

Regarding the level of Treg relative to oTL, immunoCRIT, our data consistently show immunoCRIT levels in benign tissues that range from 3 to 8% regardless of tissue type and/or natural immune privilege status (Figure 8). We found a median immunoCRIT level, for benign tissues of 3.8%. In contrast, malignant tissues (regardless of origin and immune privilege status) showed median levels of immunoCRIT of approx. 19%, with only mild fluctuations between colorectal (18.8%), bronchial (18.0%), breast (19.3%) and late stage ovarian (20.6%) cancers. Our findings show that the immunoCRIT remains stable independently of immune privilege. The large difference seen in immunoCRIT levels between benign and malignant tissues suggests that this parameter may be considered a dichotomous identification key for the detection of any malignant tissue from any healthy tissue.

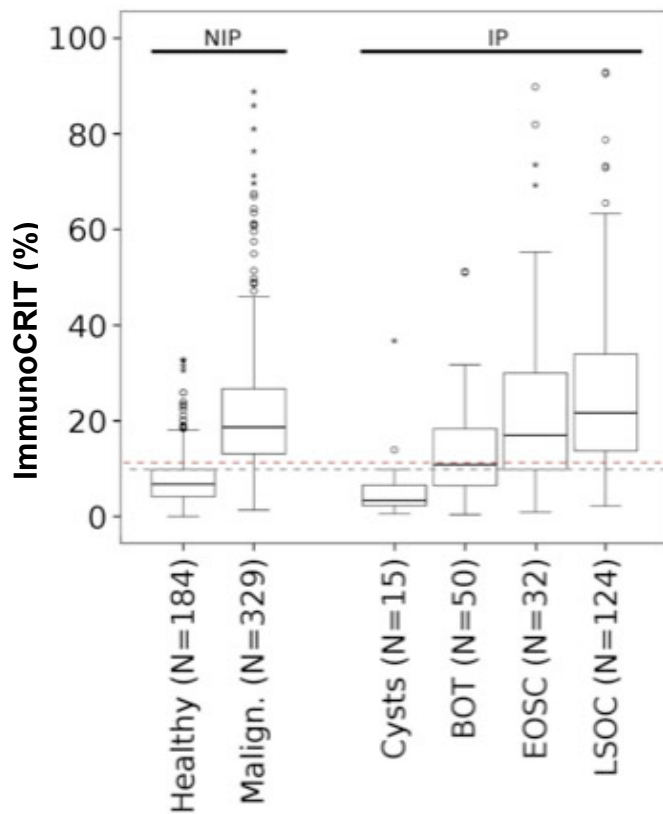


Figure 8 - Ratio of Tregs in overall T lymphocytes in tissue from healthy donors and patients with solid tumors as measured by using epigenetic FOXP3 and CD3+ demethylation assay, ratio of infiltrating Tregs and T lymphocytes in non-immune privileged (NIP) healthy and malignant (Malign.) tissues and several tissue types of immune privileged (IP) ovarian tissue (cysts, borderline ovarian tumor (BOT), early stage (ESOC) and late stage ovarian carcinoma (LSOC). Dotted lines represent the calculated cut-off values for most

accurate segregation of immune privileged healthy from malignant (green) and non-immune privileged tissues (red).

Sub-analysis of IP malignant tissues – LSOC and BOT; Correlation of disease aggressiveness with immunoCRIT in ovarian tissues

Having observed clear differences between the immunoCRIT in healthy and malignant tissues, we were interested in the correlation between immunoCRIT and malignant potential in ovarian tissue.

We first divided malignant ovarian cancer in cystadenoma, BOT, ESOC and LSOC. The immunoCRIT along the histopathologically defined disease types showed a strong shift: a median of 3.4% of overall T cells represent regulatory T cells in benign tissues. This ratio increased to 10.1% in BOT, further rising to 15.0% in ESOC and finally reaching 27.7% in LSOC. Kruskal-Wallis and Jonckheere-Testra tests indicated a highly significant group

effect as well as a gradually increasing ratio of the cellular tolerance over all stages ($p < 0.001$).

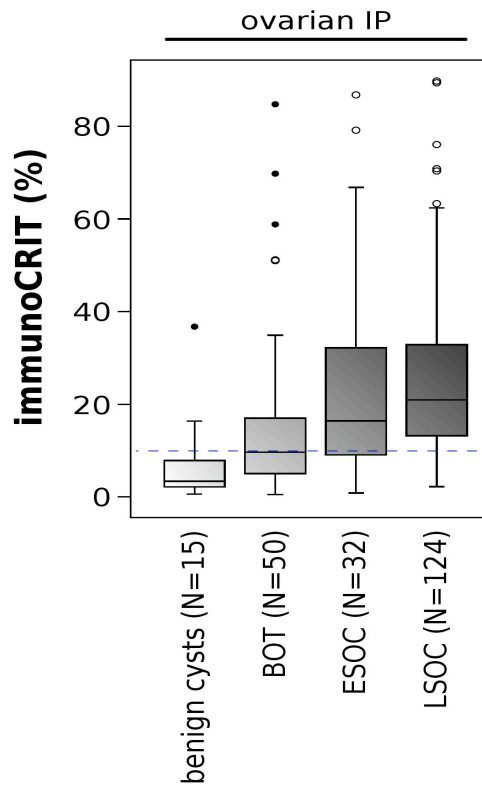


Figure 9 - Boxplot showing immunoCRIT levels in different IP ovarian tissues (cysts, borderline ovarian tumor (BOT), early stage (ESOC) and late stage ovarian carcinoma (LSOC)). Dotted line represents the calculated cut-off values for most accurate segregation between benign and malignant tissue.

More importantly, the median immunoCRIT was 10.5% for BOT without invasive implants, 8.2% for BOT with invasive implants and 27.7% for LSOC, this difference being statistically significant ($p < 0.001$, Table 8). The immunoCRIT levels in LSOC cohort significantly differ from the BOT cohorts ($p < 0.001$), while the BOT cohorts did not significantly differ between themselves (Figure 10).

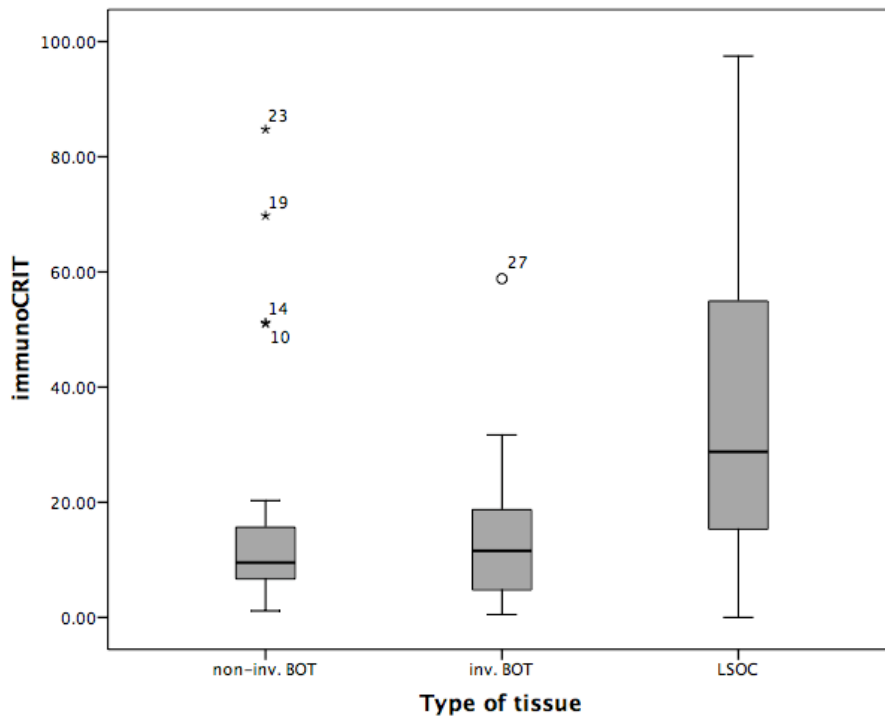


Figure 10 - Boxplot showing immunoCRIT levels in BOT without invasive implants (non-inv. BOT), BOT with invasive implants (inv. BOT) and late stage ovarian cancer (LSOC). Boxes depict the middle 50% of the distribution, the line within represents the median. Whiskers extend to include 95% of all data, mild outliers are indicated by circles, extreme outliers by stars.

Invasive and non-invasive BOT have a similar level of immunoCRIT. The mean levels are significantly higher among LSOC patients (mean 36.3%, median 27.7%) than among invasive BOT patients (mean 15.6%, median 8.2% $p=0.004$) and non-invasive BOT patients (mean 18.1%, median 10.5%, $p=0.004$). The levels between the non-invasive and invasive BOT are not significantly different.

Tissue	Cystadenoma	Non-inv. BOT	Inv. BOT	LSOC
Treg-to-oTL	3.4%	10.5%	8.2%	27.7%

Table 7 – Median immunoCRIT in the different tumorous conditions of the ovary, benign cystadenoma, BOT without invasive implants (non-inv. BOT), BOT with invasive implants (inv. BOT) and late stage ovarian cancer (LSOC)

ImmunoCRIT in peripheral blood in the cohort of patients with ovarian neoplasia

To detect whether this increase in immunoCRIT is reflected in the peripheral blood of EOC patients, we analyzed peripheral blood samples from patients with ovarian cystadenoma, BOT and EOC obtained at primary diagnosis prior to any therapy regimen. The differences in peripheral oTL levels between cystadenoma, BOT and LSOC and patients (respectively 19.3%, 16.0% and 20.3%) were minor and not statistically significant. Regarding the immuneCRIT levels, we likewise observed a similar mild, non-significant ($p = 0.22$) increase of immunoCRIT was observed when comparing blood from cystadenoma patients (median 7.44%) with that from BOT and LSOC patients (median 8.0% and 8.55%, respectively).

ImmunoCRIT in peripheral blood in the disease course of EOC patients

Our finding that malignant tissues show a high immunoCRIT, together with the fact that the immune system is generally incapable of clearing recurrent malignant tumors under therapy, prompted us to analyze peripheral cellular tolerance in the disease course of LSOC patients. For this, we monitored the immunoCRIT in the peripheral blood at different time points of

disease progress in 10 patients (all patients from our cohort for whom there were available blood samples at different time points) by measuring epigenetic cell typing assays for regulatory T cells, overall T-lymphocytes as well as assays for the T cell subpopulations of T helper (CD4 assay) and cytotoxic T cells (CD8B assay) as confirmation for the overall T cell assay. In order to obtain a homogeneous cohort of LSOC patients, only patients with a histologically confirmed late stage epithelial ovarian cancer of serous histopathology and at least one recurrence were included. Patients of non-serous histology as well as early stage and low-grade cancer were excluded from this analysis. These patients were FIGO stage IIIB (1) and IIIC (9) and were treated at the Clinic for Gynecology and Obstetrics, Charité Campus Virchow (Berlin) between 10/12/2003 and 5/18/2012. During the follow-up period, 7 patients succumbed to the disease. For all patients the first line of treatment was based on a platinum-taxol chemotherapy regimen, whereas 2nd, 3rd and 4th line therapies varied between patients. The age of patients at initial diagnosis ranged from 41 to 74 and median age was at 57 years. For 8 patients, the first blood draw used in the current analysis was at initial diagnosis, whereas for the remaining 2 the first blood draw was performed 6 months after initial diagnosis (patient No.10) and at first recurrence (patient No. 5, i.e., 27 months after initial diagnosis). The time points selected to monitor the immunoCRIT in the course of disease include blood draws at disease recurrence. In three cases, we also monitored time points at regular aftercare blood draws, i.e., between two disease events.

Pat #	Event	Age at initial diagnosis (ID)	Histopath.	FIGO	Time after ID (month)	Treg (%)	oTL (%)	Cellular Tolerance (%)	
1	Initial Diagnosis				0	7,6	11,1	68,0	
	Aftercare	65	serous	3c	14	2,1	22,8	9,1	
	Relapse 3				26	1,1	11,4	9,4	
	Relapse 4				33	1,3	5,2	25,0	
Initial diagnosis	0				0,9	6,6	13,5		
2	Aftercare	50	serous	3c	13	2,5	15,7	15,9	
	Relapse #1				35	1,0	4,5	22,3	
3	Initial diagnosis	66	serous	3c	0	1,9	17,9	10,4	
	Relapse 1				7	1,3	11,8	11,3	
4	Initial diagnosis	74	serous	3c	0	1,8	11,0	16,0	
	Relapse 1				13	1,6	9,1	17,1	
5	Relapse 1	41	serous	3c	27	0,8	14,9	5,6	
	Relapse 3				51	1,6	15,5	10,4	
6	Initial diagnosis	61	serous	3b	0	1,8	15,0	12,1	
	Relapse 1				20	1,5	9,5	15,4	
	Relapse 3				52	2,4	12,8	19,1	
7	Initial diagnosis	57	serous	3c	0	1,1	8,5	12,6	
	Relapse 1				21	0,9	5,6	15,6	
8	Initial diagnosis	51	serous	3c	0	1,6	13,5	12,1	
	Relapse 1				44	1,6	10,5	15,5	
	Relapse 2				67	1,9	13,3	13,9	
9	Initial diagnosis	68	serous	3c	0	0,8	3,4	22,9	
	Relapse 1				13	1,4	11,5	12,2	
10	Aftercare	57	serous	3c	6	2,4	14,4	17,0	
	Relapse 1				13	1,9	10,3	17,9	

Table 5 – Characteristics of the patients, blood-draw time points, Treg, oTL and Cellular Tolerance (ImmunoCRIT) levels measured in the peripheral blood of LSOC. Green arrows indicate rising levels of cellular tolerance through disease progression, the yellow arrow indicates a stable level cellular tolerance and the red arrow indicates falling levels of cellular tolerance through disease progression.

Relative Treg and oTL cell numbers at time points measured first, mostly at initial diagnosis, were in the previously observed range (0.8 to 7.6% and 3.4% to 22.8%, median 1.5% and 11.5%, respectively) and did not show any trend of correlation with disease progression. As expected, the overall T-lymphocytes cell values showed high correlation (Spearman's rho=0.999) to combined CD4 and CD8 cell numbers, except for Pat. #1, who showed a biologically utterly implausible discrepancy at initial diagnosis (Figure 11).

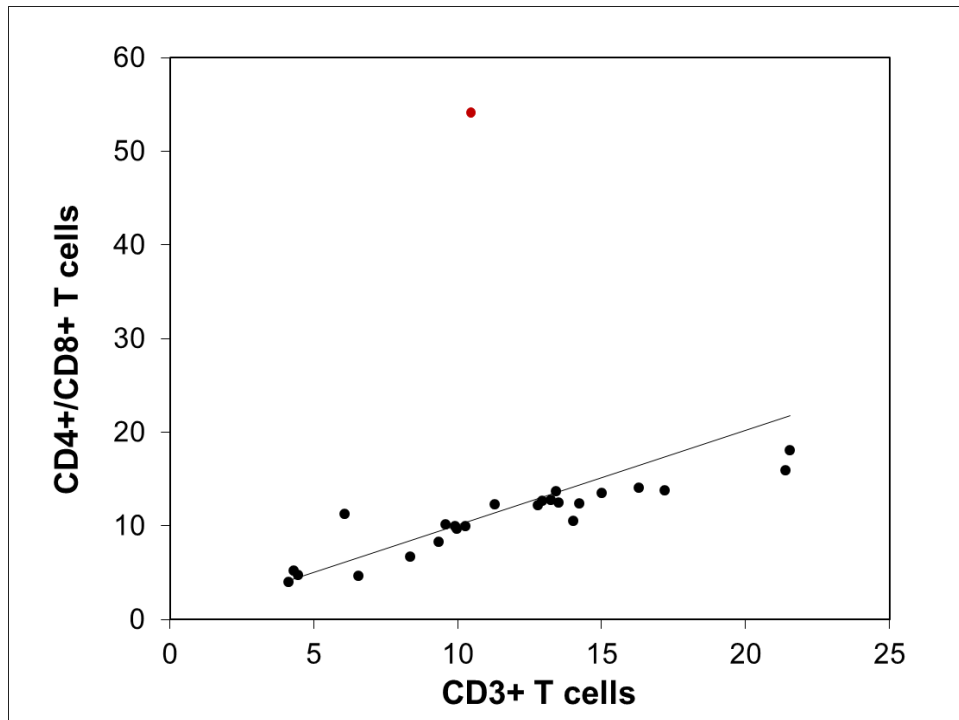


Figure 11 – Spearman correlation between CD3+ and CD4+/CD8+ T cells. Patient #1 is represented in red as an outlier, showing a biologically implausible discrepancy between CD3 and CD4/CD8 levels.

In line with our assumption, we observed a strong increase of peripheral immunoCRIT along with disease progression. In 8 out of 10 patients, the initially detected values were constantly lower than the immunoCRIT at later time points. In one patient (#8) this was principally confirmed since the immunoCRIT level at the initial diagnosis was lower when compared to both later time points, but this level was highest at the first relapse rather than at the second one. Another patient (#1) also showed the expected increase starting from aftercare relapse 1 over relapse 3 through relapse 4, but she represents the aforementioned outlier at initial diagnosis with respect to CD3 T cell and T helper/cytotoxic T cell correlation ratio. Hence, for this patient we considered the expected increasing trend to be confirmed. Finally, one patient (Pat #9) appeared to have a reduction of

immunoCRIT levels when comparing the initial diagnosis to the relapse. It is noteworthy that the observed T cell value was at a pathologically low level at initial diagnosis, both by CD3 oTL and combined CD4 and CD8 cell count analysis. Including all data points by applying the Page trend test ($p=0.01$), we find the increase of cellular tolerance along with the progress of disease statistically significant.

Summary of most prominent findings

From our study the central findings allowing us to discuss the transcoelomic pattern of metastasis characteristic for ovarian tumors can be summarized as follows:

- The central difference between IP and NIP tissues are the levels of infiltrating oTL
- All malignant states show increased levels of immunoCRIT regardless of immune privilege
- The immunoCRIT levels in the peripheral blood of patients with ovarian cysts, BOT and ovarian cancer are comparable and comparable to their healthy counterpart
- In ovarian cancer disease progression with appearance of distant metastasis correlates with high peripheral levels of immunoCRIT

Discussion

Establishment of malignant tumors depends on favorable growth kinetics¹⁰⁴ of tumor cells and their strategies to evade immune surveillance²³. Even though both BOT and EOC are considered malignant diseases derived from the same tissue and cell-type, they are characterized by different, almost opposite, clinical behavior. Even today BOT remain one of the most controversial topics, confusing both clinicians and patients, as the category has often led to both inadequate treatment and overtreatment. Due to the similar cellular origin of EOC and BOT, they appear to be an appropriate substrate to analyze the role the immune system plays in the disease outcome. Even though BOT are regarded as malignant, they usually present a benign behavior, while some patients suffer relapses and develop progressive disease. At present, apart from the presence of invasive implants and residual disease after up-front surgery^{45,105}, there is no marker capable of predicting the outcome, posing a clinical problem. Micropapillary patterns and stromal micro-invasion in serous BOT and intraepithelial carcinoma in mucinous BOT remain controversial factors¹⁰⁵. The current study analyzed the relative amount of different tumor-infiltrating lymphocytes subtypes in these tumors, aiming to examine a possible immunological explanation for this difference in their clinical behavior.

Characteristics of the cohort

To our knowledge, this is the first study to examine the role of immunological cell shifts and the prognostic influence of different tumor-infiltrating lymphocytes in both invasive and non-invasive BOT, and to compare them to EOC and other NIP malignancies. The study benefits from a large cohort of invasive BOT samples and from a large cohort of homogeneously treated EOC patients. However, the follow-up was relatively short, particularly for BOT, a disease characterized by its protracted course.

EOC FIGO Stage I (ESOC) patients were considered in a different subgroup because the prognosis of early-stage patients significantly differs from late-stage patients. In our LSOC cohort all patients were homogeneously treated with adjuvant chemotherapy, consisting of 6 cycles of carboplatin (75mg/m² over 30 minutes) plus paclitaxel (175mg/m² over a three-hour period). Grade I EOC patients constitute a mere 1.9% of our cohort and should not influence the result even if currently believed to arise in a stepwise fashion from a cystadenoma or a borderline tumor, whereas high-grade neoplasms are considered *de novo* lesions⁶³⁻⁶⁵.

The distribution of the EOC patients by stage in the current study is in accordance with the worldwide distribution of ovarian cancer by stage at presentation⁸⁵. The distribution of histological sub-type is concurrent with the expected distribution, as is the survival rate and the mean progression-free survival⁷⁴. Overall, the present cohort can be regarded as being a representative sample of the usual ovarian cancer population.

The cohort of BOT patients was relatively youthful, with a mean age of 48 years, as expected in BOT patients. With 12 patients presenting with invasive implants, this is a considerably large cohort with invasive implants^{83,106}. However, the mean duration of follow-up of 28.66 ± 32.09 months is short, considering that BOT is a slow-developing disease. There were only 3 (6.0%) deaths and 12 (24.0%) recurrences within the follow-up period, mostly limited to patients with invasive implants reflecting the overall good prognosis of this disease in the absence of invasive implants⁸².

Taken together, these cohorts are appropriate for this study, since they consist of an average mostly high-grade, late stage EOC cohort that considers stage I tumors separately and a particularly solid BOT cohort that includes a large group of patients with invasive implants, which are known to occur seldom.

Tumor infiltrating lymphocytes

Overall T lymphocytes – CD3 marker

The presented data along with previous data¹⁶ (which also employed epigenetic T-cell quantification) demonstrate that ovarian tissue, cancerous or not, shows a very low infiltration of immunological cells when compared to other tissues, hence qualifying as an immune privileged site. It was demonstrated that ovarian cystadenoma show a median oTL infiltration of 3.9%, whereas healthy bronchial tissue shows 29.6% and colorectal tissue shows 33.5% infiltration¹⁶. In the present study the mean oTL levels for the

non-invasive BOT cohort were 4.7% (median 3.0%), significantly lower than the mean oTL levels for the invasive BOT cohort (10.9%, median 8.9%, $p=0.028$) and LSOC cohort (10.2%, median 7.3%, $p=0.001$). It is worth noting that the mean levels of oTL in non-invasive BOT cohort are comparable to those of cystadenoma (Table 5). These consistently low immune cell levels show that the ovary is an immune-privileged site (IP) and it was further shown that higher levels of oTL, compared to their benign counterparts, characterize malignancy states in these IP tissues.

This finding is not common to other tumor entities deriving from NIP tissues. In lung and colorectal cancers, for instance, oTL levels are shown to be reduced, probably because healthy samples of these tissues show high oTL levels^{16,107}. Bronchial cancer shows levels of 22.3% oTL, while colorectal cancer shows levels of 26.1% oTL (healthy tissue shows 29.6% oTL and 33.5% oTL, respectively). Our study shows that instead, LSOC presents double the levels of oTLs shown in healthy ovarian tissue. Given that T-lymphocyte frequencies are lower in healthy ovarian tissue than in other tissues, this probably reflects the fact that enhanced oTL-levels are due to tumor-mediated increase of stroma density and neo-angiogenesis (Table 6). As shown, infiltration of overall T-lymphocytes increases from ESOC (4.3%) to LSOC (7.3%) and this may reflect no more than tumor-induced neoangiogenesis together with an accumulation of T-cells bearing tumor associated antigen receptors. We observed an opposite trend in all non-immune privileged tissues, where malignant tumors show a reduction of the overall T-cell share compared to their healthy counterparts. In this case, this may simply reflect the exponential growth of tumor cells without an equally fast immune cell accumulation. When comparing NIP and IP, however, the

orientation of T cell infiltration change is not a uniform denominator of tumor development. Nevertheless, in both NIP and IP tissues, tumor development leads to a distorted overall T- cell balance and the difference in the status of immune privilege is undermined in tumorigenesis of all analyzed tissues.

The presence of invasive disease in BOT cases seems to result in a pattern of oTL considerably more similar to LSOC than to non-invasive BOT. One possible explanation would be that invasion plays a role in triggering the process of angiogenesis necessary for the supply of oxygen and nutrients for tumor growth, or that angiogenesis is a required step for transition from a cluster of atypical cells to stromal invasion. In non-invasive BOT the low oTL levels are comparable to healthy ovarian tissue, hence following our line of thought, the vascularization would be within the normal range for this tissue. On the other hand, in other tumors such as bronchial and colorectal cancer, where there is no major difference between healthy and diseased tissue, the number of oTL probably corresponds to the ability of the immune system to recognize and respond to the tumor. By contrast the high number of oTLs seen in ovarian tissue are a consequence of enhanced vascularization due to neo-angiogenesis. Studies of EOC tissue show results consistent with our own, with a high-density of CD3+ T cells in tumor epithelium^{16,108,109}. One previous study analyzed the levels of Id-1, a protein essential to the vascularization of tumors, in BOT and EOC and reported that the expression of Id-1 was found significantly more often in EOC than in BOT and benign cysts¹¹⁰. Another study analyzed the significance of vascular endothelial growth factor in benign cysts, BOT and EOC and found that expression levels with the correlated with diagnosis, being higher for EOC¹¹¹.

Regulatory T cells – FOXP3 marker

Regarding Treg, it was shown that cystadenoma show a mean infiltration of 0.1%, while healthy bronchial tissue shows a value of 2.0% and colorectal tissue 1.9%¹⁶. Regardless of immune privilege, benign tissues show consistent similar levels of Treg.

In the present study, the mean Treg value of 1.4% for the invasive BOT cohort is three times higher than the Treg levels in the non-invasive BOT group (0.5%, $p=0.006$), while the value of 2.3% is approximately 5 times higher in the LSOC cohort ($p<0.0005$). Even in non-invasive BOT the Treg levels are approximately 4 times higher than the levels previously established in healthy ovarian tissue¹⁶ (Table 7).

There is a trend towards an immunological failure with disruption of the immune system in LSOC that establishes an immunosuppressive state within the tumor microenvironment. This suggests that EOC cells may release chemokines and cytokines that create an immunosuppressive microenvironment as an escape strategy, a strategy that is neither evident in non-invasive nor in invasive BOT. This could be one possible explanation for why 16.7% of patients with invasive BOT died, compared to 32.0% of patients with ovarian cancer: the tumor cells in invasive BOT patients are in a better equilibrium with the host's immune system, whereas in LSOC, the high levels of Treg act as an escape mechanism in the immune competent host. As mentioned, only one of the patients with non-invasive disease died. In a previous study, Treg were shown to accumulate preferentially in the tumor

mass relative to draining lymph nodes¹⁷, corroborating the hypothesis that the tumor microenvironment is able to induce an immunosuppressive state as an evasion strategy. One of the proposed mechanisms underlying this phenomenon is the presence of the chemokine CCL22, secreted by tumor cells and tumor-associated macrophages, which binds to CCR4 expressed on Treg and creates a concentration gradient that mediates the migration of Treg towards the CCL22-rich tumor microenvironment. Indeed, high expression levels of FOXP3 have been shown to represent an independent prognostic factor for ovarian cancer^{112,113}. Similar findings regarding Treg trafficking and redistribution have been reported in various types of malignancies, such as breast cancer^{113,114}, carcinomatous meningiosis¹¹⁵ and lung cancer¹¹⁶. Treg were found to be elevated in a wide range of malignant diseases and to correlate with a negative prognosis, such as breast¹¹⁷, pancreatic¹¹⁸, hepatocellular¹¹⁹ and gastric cancer¹²⁰. Nonetheless, it is important to take into consideration that a considerable number of these studies were carried out during the period when the phenotype of Treg was being refined, thereby limiting direct comparisons between studies. Furthermore, different laboratory techniques and methods, such as mRNA, immunohistochemistry or qPCR, were used to determine the levels of Tregs, hindering direct comparisons.

Cellular Ratio of Immune Tolerance - Ratio of regulatory T cells relative to the percentage of overall T lymphocytes:

immunoCRIT in NIP and IP tissues, non-invasive and invasive BOT, and proposed model for metastatic spread

The ratio of Treg relative to the overall population of T lymphocytes and here referred to as immunoCRIT was determined in order to assess the immune status, excluding the vascularization-associated factor. In accordance with our previous publication, immunoCRIT is again found to be relatively stable throughout all healthy tissues independent of origin and immune privilege status (app. 3-8%), despite significant differences in T cell infiltration levels¹⁶. A consistent increase in immunoCRIT is observed throughout all tumor entities compared to their respective benign counterparts, which supports previous findings that active cell-mediated tolerance in the tumor microenvironment is a central mechanism of immune escape of solid cancers.

In this aspect, invasive and non-invasive BOT appear to have a similar level of immunoCRIT (Figure 12). Indeed, the mean immunoCRIT is significantly higher among LSOC patients (36.3%, median 27.7%) than the mean for the invasive BOT group (15.6%, median 8.2% $p=0.004$) and non-invasive BOT group (18.1%, median 10.5%, $p=0.004$). The levels are not significantly different between the non-invasive and invasive BOT.

The central difference between invasive and non-invasive BOT is the oTL levels (3,02% and 8,78% $p=0.028$). When moderately elevated immunoCRIT levels (translating an immunosuppressive state that allows tumor cell escape) constituted by an absolute low number of cells (low oTL) meet normal peripheral levels of immunoCRIT, these would normalize

immunoCRIT levels allowing tumor elimination. This is the case in non-invasive BOT (Figure 12). On the other hand, in the case of invasive BOT, the moderately elevated immunoCRIT levels constitute a high absolute number of cells (high oTL levels). When these cells encounter normal peripheral immunoCRIT levels, the later are overcome and the tumor is further allowed to escape immune surveillance. The consequences are reflected in the different outcome of the cohorts with respectively 5,3% recurrence rate and 100% survival rate, compared to 83% recurrence rate and 75% survival rate at 2 years.

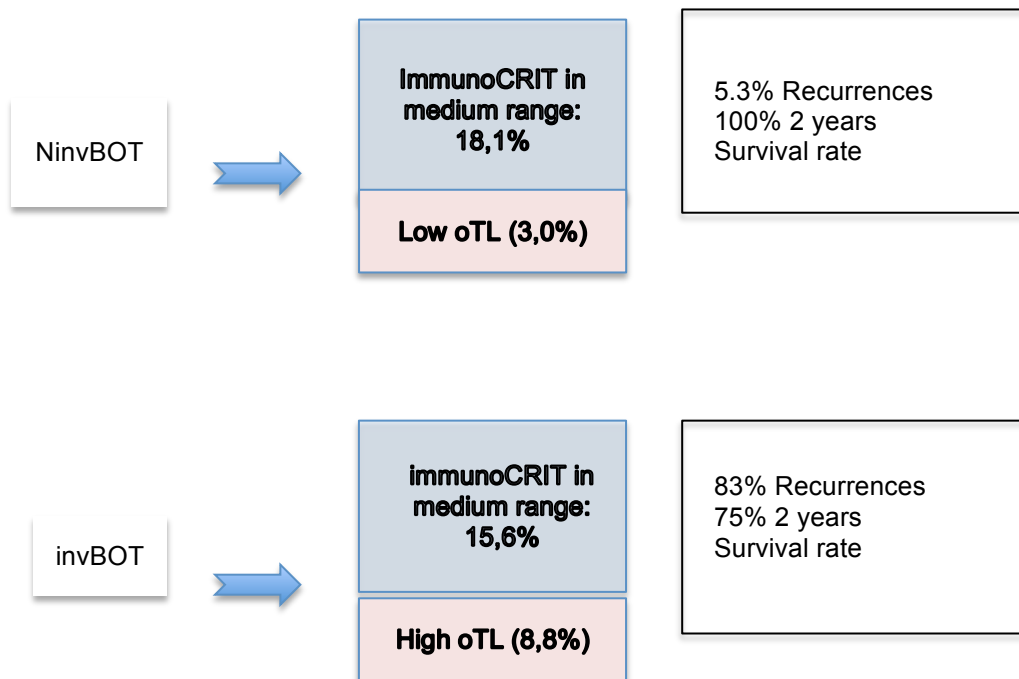


Figure 12 – The proposed central difference in non-invasive and invasive BOT resides in their absolute levels of oTL, that are (or not) counteracted by normal peripheral immunoCRIT levels.

As evidenced by its immunoCRIT, only LSOC is shown to have the capacity to disrupt the immune system, establishing an immunosuppressive state within the tumor microenvironment capable of synergistically supporting

cell proliferation as an escape strategy. The increase in Treg levels and - as a consequence - in immune tolerance, supports the observation that tumors promote immune-escape throughout accumulation of Tregs in their microenvironment. This consistent observation through all tested tumor entities suggests that increases in cellular tolerance are a requirement for tumor development. It is a constant finding across malignant states, regardless of immune privilege, that these show high immunoCRIT levels. The central difference resides in the absolute number of immune cells, that is, oTL. Similar to what previously postulated for BOT tumors, when NIP tissues with manifestly high levels of immunoCRIT (19.0% for NIP tissues) constituted by a high absolute number of cells (high oTL: 21,6% for NIP) come to contact with normal peripheral immunoCRIT levels, they cause a shift in the peripheral immunoCRIT leading to its increase and allowing tumor escape and hematogenous spread. In contrast in IP tissues these high levels of immunoCRIT (20.6% for LSOC tissues) are constituted by a low absolute number of cells (low oTL: 7,3% for LSOC) that become "diluted" by a peripheral normal immunoCRIT allowing immunological elimination of tumor cells and avoiding hematogenous spread. Only in the course of the disease, tumor induced peripheral increased immunoCRIT levels allow the tumor to overcome surveillance and spread through the blood (Figure 13).

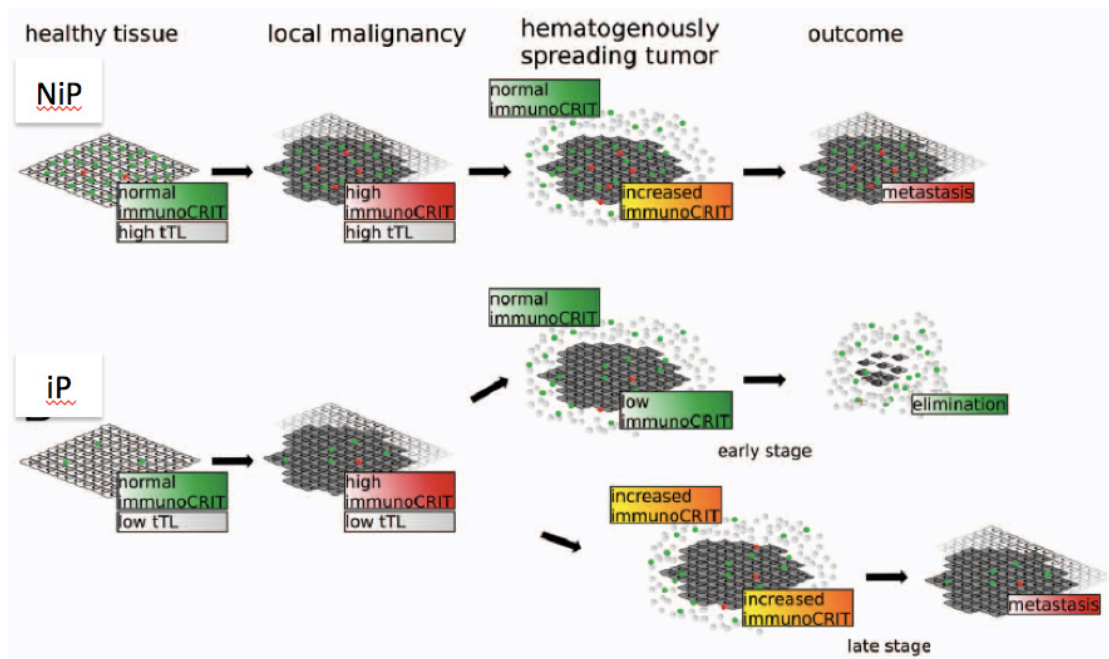


Figure 13 – Schematic representation of NIP and IP malignancies interaction with peripheral immunoCRIT, allowing either tumor escape with metastatic disease (NIP and LSOC), or tumor elimination (ESOC)

It is well known that in the setting of cancer, dendritic cells are involved in the peripheral generation of Treg, because dendritic cells exposed to tumor cells acquire an immunosuppressive phenotype associated with the induction of Treg²⁴. Ovarian cancer cells have been shown to produce TGF- β , which suppresses the activity of oTL and converts effector T-cells into Treg¹²¹. Tumor-associated plasmacytoid dendritic cells were shown to induce Treg¹²² and tumor-induced indoleamine 2,3-dioxygenase directly enhances local Treg-mediated immunosuppression¹²³. Furthermore, CCL22 causes Treg migration into tumors, and is found at high levels in tumor ascites of patients with EOC¹⁷. It has been demonstrated that a high CD8+/Treg ratio correlates with a favorable prognosis in ovarian cancer¹²⁴. Furthermore, it has been shown that a high oTL-to-Treg ratio in tumor-containing ovarian tissue correlates with a longer disease free survival¹⁶. Analysis of the shift of the

Treg-to-oTL ratio was shown to be linked to tumor burden and disease course in several cancers such as hepatocellular carcinoma¹²⁵, cervical cancer¹²⁶ and lung cancer¹²⁷.

ImmunoCRIT in the peripheral blood of patients with ovarian neoplasia and dissemination patterns dependent on NIP vs. IP tissues

When analyzing the oTL counts and the immunoCRIT values in peripheral blood of healthy subjects, patients with BOT and patients with LSOC, there were neither statistically relevant differences in the oTL counts nor in the immunoCRIT values.

Our data show that the median oTL counts in malignant NIP tissue samples (20.6%) were not significantly different from the corresponding values in the peripheral blood of healthy donors (20.1% $p=0.495$). Accordingly, the oTL count in ovarian tissue samples (cystadenoma 3.9% and EOC 7.3%) was significantly lower than peripheral oTL counts in blood from either healthy donors ($p<0.001$) or EOC patients ($p<0.001$). Being an IP site with low levels of tissue immune cells, such limited effect of the tumor on the peripheral immune system is not surprising.

Regarding the immunoCRIT, it is elevated in tissues when compared to peripheral blood, both from cancer patients and healthy donors. Notably, the absence of Treg-mediated tolerance coincides with a general absence of peripherally disseminated metastases at PD of ovarian cancer, whereas tumors derived from NIP tissues more often show hematogenous spread into distant organs. Extra-abdominal metastases in ovarian cancer pose a more frequent problem in later stages of disease, i.e., upon recurrence and

treatment. We assume that the peripheral immunoCRIT levels may rise in the course of disease until, eventually, peripheral tolerance is sufficient to foster hematogenous tumor spread. To test this hypothesis, we analyzed ovarian cancer patients under treatment over their courses of disease. We observed a highly significant correlation of immunoCRIT over disease course in the periphery. These data indicate that ovarian cancers do exhibit a strong tolerance-inducing effect in the periphery, coinciding with the higher likelihood of extraperitoneal metastases.

While no causal evidence can be derived from the present data, one may speculate that the absence of increased cellular tolerance in the periphery, along with the comparable low presence of dysbalanced cellular tolerance in the tumor microenvironment and its metastasizing clones, may explain the lower likelihood of ovarian neoplasms to metastasize via the hematogenous route.

ImmunoCRIT in peripheral blood in the course of LSOC patients

When analyzing levels of immunoCRIT in the periphery of healthy subjects of patients with BOT and those with LSOC, no statistically relevant differences in overall T cell counts or immunoCRIT were seen. Considering the low levels of immune cell infiltration observed in ovarian tissue, this lack of a clear increase in peripheral tolerance may be expected and is consistent with a lack of distant metastatic disease. Whereas extra-abdominal metastases are rarely found at initial diagnosis of LSOC, they do occasionally occur when patients experience repeated recurrences and therefore we opted

to analyze relapsing ovarian cancer patients under treatment over their course of disease.

A highly significant correlation of immunoCRIT with disease progression was found, seen in the periphery of 8 of 10 patients. In at least two cases, the increase of immunoCRIT was also in parallel with development of extra-abdominal metastases. The epigenetic data of the CD3+ T lymphocytes were also confirmed by an independent measurement of CD4+ and CD8+ T cells. With the exception of one peculiar, unexplained outlier, the sum of both latter measurements strictly correlated with the detected number of overall T lymphocytes, indicating that the measurements were technically and biologically sound. However, whereas these data stress the validity of these findings, no functional studies were conducted. Thus, it remains unresolved whether immunoCRIT and tumor progression are directly and functionally dependent on each other. Thus, despite high statistical significance of the observed trend, future studies with a larger cohort should be conducted. If a functional relation is confirmed, immunoCRIT may provide a new target point of strategies to contain disease progression.

Concluding Remarks

The ovaries repeatedly show low levels of immune cell infiltration and are therefore considered immune privileged sites. Within the ovaries several conditions of epithelial proliferation may occur resulting in a wide spectrum of disease courses, as is the case in cystadenoma, borderline ovarian tumors and epithelial ovarian cancer. Borderline tumors in particular remain a clinical challenge for clinicians and a confusing diagnosis for patients.

In these conditions, the immune profile within the ovarian tissue changes, along with the malignant potential. On the one hand, high levels of oTL in invasive BOT and LSOC when compared to non-invasive BOT and cystadenoma hint that neo-angiogenesis and consequently an increase in vascularization appear to be related to the event of stromal invasion. These are able to counteract normal peripheral levels of immunoCRIT allowing disease progression. In contrast, in non-invasive BOT the low levels of oTL allow peripheral dampening of moderately elevated immunoCRIT levels and tumor cell elimination as well as damping of vascular formation.

The Treg levels, representing a surrogate marker for an immunosuppressive milieu by contributing to immune escape, on the other hand, are higher for non-invasive BOT when compared to cystadenoma; they then triple in BOT with invasive implants and finally are 5 times higher in LSOC. A shift toward higher immunoCRIT is prerequisite to tumor growth in all tissues regardless of oTL count and immune privilege. The ability to invade local tissues becomes more pronounced along with elevated immunoCRIT values. Transceolomic spread proceeds without overcoming immunological barriers. However, for hematogenous spread tumors need to overcome the peripheral immune environment. The immunoCRIT levels in healthy blood are

at approx. 5% and thus significantly lower than in tumorous tissue (approx. 20%). The percent share of oTLs in non-immune privileged tissues is nearly equivalent to the bloodstream. In ovarian tissue oTL infiltration is significantly lower. The immunoCRIT in the microenvironment of the hematogenously circulating tumor lump is reduced to a non-pathological level by the low immunoCRIT in the surrounding bloodstream, allowing its elimination. Hence, tumor expansion remains confined to the abdominal cavity. If higher peripheral tolerance along the course of disease is established immunoCRIT in the microenvironment of the circulating tumor structure remains high and metastases evade elimination even outside the abdomen. The same applies for BOT, where the only difference between invasive and non-invasive BOT is the oTL - in non-invasive BOT oTL infiltration being significantly lower.

By evaluating samples of non-invasive BOT, invasive BOT and EOC, the data support the view that the imbalance between tolerogenic and effector immune cells is a characteristic of tumor establishment. These data are consistent with our assumption that there is a strict correlation between the aggressiveness of disease and infiltrating immune cells. Whereas a molecular correlation between malignant cell type and aggressiveness of disease has not been established yet, we are able to show a compelling agreement between tumor infiltrating immune cell types and numbers and disease behavior.

In the hope of shedding light on the particular transcoelomic spreading pattern of EOC we analyzed the immune profile seen in the peripheral blood of healthy donors and in patients with these different ovarian neoplasia. The median oTL levels in the peripheral blood of healthy donors were similar to the levels seen in malignant NIP tissues, and much higher than the levels

seen in ovarian tissues, malignant or not. Regarding the immunoCRIT, it is much higher in cancerous ovarian tissue when compared to its healthy counterpart and peripheral blood, both from cancer patients and healthy donors. The absence of increased cellular tolerance in the periphery along with the comparable low presence of dysbalanced cellular tolerance in the tumor microenvironment and its metastasizing clones may explain the lower likelihood of ovarian neoplasms to metastasize via hematogenous route.

Finally, because hematogeneous spread does occur later in recurrent disease, we analyzed the peripheral blood of LSOC patients in its course. Disease progression was reflected in the peripheral immunoCRIT. This finding needs to be confirmed by a larger cohort. If confirmed, therapies such as intraperitoneal transfusion of autologous peripheral blood T lymphocytes, as an attempt to re-establish immunoCRIT levels in the tumor environment, could be considered as therapeutic approaches.

Literature References

1. Medzhitov R, Janeway CA, Jr. Decoding the patterns of self and nonself by the innate immune system. *Science*. Apr 12 2002;296(5566):298-300.
2. Mayer G. Immunology Section of Microbiology and Immunology Online. 2011; <http://pathmicro.med.sc.edu/ghaffar/innate.htm>.
3. Alberts BAJ, Julian Lewis, Martin Raff, Keith Roberts, and Peter Walters *Molecular Biology of the Cell*. London and New York 2002.
4. Pier GB LJ, Wetzler LM *Pilmmunology, Infection, and Immunity*. 2004.
5. Kindt T, Osborne B, Goldsby R. *Kuby Immunology*. 6th ed: W. H. Freeman; 2006.
6. Apostolou I, Sarukhan A, Klein L, von Boehmer H. Origin of regulatory T cells with known specificity for antigen. *Nat Immunol*. Aug 2002;3(8):756-763.
7. Tan DS, Agarwal R, Kaye SB. Mechanisms of transcoelomic metastasis in ovarian cancer. *Lancet Oncol*. Nov 2006;7(11):925-934.
8. Shankaran V, Ikeda H, Bruce AT, et al. IFN γ and lymphocytes prevent primary tumour development and shape tumour immunogenicity. *Nature*. Apr 26 2001;410(6832):1107-1111.
9. Schreiber RD, Old LJ, Smyth MJ. Cancer immunoediting: integrating immunity's roles in cancer suppression and promotion. *Science*. Mar 25;331(6024):1565-1570.
10. Matzinger P. Tolerance, danger, and the extended family. *Annu Rev Immunol*. 1994;12:991-1045.
11. San Jose E, Sahuquillo AG, Bragado R, Alarcon B. Assembly of the TCR/CD3 complex: CD3 epsilon/delta and CD3 epsilon/gamma dimers associate indistinctly with both TCR alpha and TCR beta chains. Evidence for a double TCR heterodimer model. *Eur J Immunol*. Jan 1998;28(1):12-21.
12. Szabo SJ, Sullivan BM, Peng SL, Glimcher LH. Molecular mechanisms regulating Th1 immune responses. *Annu Rev Immunol*. 2003;21:713-758.
13. Khong HT, Restifo NP. Natural selection of tumor variants in the generation of "tumor escape" phenotypes. *Nat Immunol*. Nov 2002;3(11):999-1005.
14. Dunn GP, Old LJ, Schreiber RD. The three Es of cancer immunoediting. *Annu Rev Immunol*. 2004;22:329-360.
15. Vesely MD, Kershaw MH, Schreiber RD, Smyth MJ. Natural innate and adaptive immunity to cancer. *Annu Rev Immunol*. Apr 23;29:235-271.
16. Sehouli J, Loddenkemper C, Cornu T, et al. Epigenetic quantification of tumor-infiltrating T-lymphocytes. *Epigenetics*. Feb 1 2010;6(2):236-246.
17. Curiel TJ, Coukos G, Zou L, et al. Specific recruitment of regulatory T cells in ovarian carcinoma fosters immune privilege and predicts reduced survival. *Nat Med*. Sep 2004;10(9):942-949.
18. Galon Jrm, Costes A, Sanchez-Cabo F, et al. Type, Density, and Location of Immune Cells Within Human Colorectal Tumors Predict

- Clinical Outcome. *Science*. September 29, 2006 2006;313(5795):1960-1964.
19. Woo EY, Chu CS, Goletz TJ, et al. Regulatory CD4(+)CD25(+) T cells in tumors from patients with early-stage non-small cell lung cancer and late-stage ovarian cancer. *Cancer Res*. Jun 15 2001;61(12):4766-4772.
 20. Liyanage UK, Moore TT, Joo HG, et al. Prevalence of regulatory T cells is increased in peripheral blood and tumor microenvironment of patients with pancreas or breast adenocarcinoma. *J Immunol*. Sep 1 2002;169(5):2756-2761.
 21. Clemente CG, Mihm MC, Jr., Bufalino R, Zurrada S, Collini P, Cascinelli N. Prognostic value of tumor infiltrating lymphocytes in the vertical growth phase of primary cutaneous melanoma. *Cancer*. Apr 1 1996;77(7):1303-1310.
 22. Naito Y, Saito K, Shiiba K, et al. CD8+ T cells infiltrated within cancer cell nests as a prognostic factor in human colorectal cancer. *Cancer Res*. Aug 15 1998;58(16):3491-3494.
 23. Dunn GP, Bruce AT, Ikeda H, Old LJ, Schreiber RD. Cancer immunoediting: from immunosurveillance to tumor escape. *Nat Immunol*. Nov 2002;3(11):991-998.
 24. Ghiringhelli F, Puig PE, Roux S, et al. Tumor cells convert immature myeloid dendritic cells into TGF-beta-secreting cells inducing CD4+CD25+ regulatory T cell proliferation. *J Exp Med*. Oct 3 2005;202(7):919-929.
 25. Akasaki Y, Liu G, Chung NH, Ehtesham M, Black KL, Yu JS. Induction of a CD4+ T regulatory type 1 response by cyclooxygenase-2-overexpressing glioma. *J Immunol*. Oct 1 2004;173(7):4352-4359.
 26. Fiore F, Nuschak B, Peola S, et al. Exposure to myeloma cell lysates affects the immune competence of dendritic cells and favors the induction of Tr1-like regulatory T cells. *Eur J Immunol*. Apr 2005;35(4):1155-1163.
 27. Sakaguchi S, Sakaguchi N, Asano M, Itoh M, Toda M. Immunologic self-tolerance maintained by activated T cells expressing IL-2 receptor alpha-chains (CD25). Breakdown of a single mechanism of self-tolerance causes various autoimmune diseases. *J Immunol*. Aug 1 1995;155(3):1151-1164.
 28. de la Rosa M, Rutz S, Dorninger H, Scheffold A. Interleukin-2 is essential for CD4+CD25+ regulatory T cell function. *European Journal of Immunology*. 2004;34(9):2480-2488.
 29. Itoh M, Takahashi T, Sakaguchi N, et al. Thymus and autoimmunity: production of CD25+CD4+ naturally anergic and suppressive T cells as a key function of the thymus in maintaining immunologic self-tolerance. *J Immunol*. May 1 1999;162(9):5317-5326.
 30. Baecher-Allan C, Brown JA, Freeman GJ, Hafler DA. CD4+CD25high regulatory cells in human peripheral blood. *J Immunol*. Aug 1 2001;167(3):1245-1253.
 31. Bennett CL, Christie J, Ramsdell F, et al. The immune dysregulation, polyendocrinopathy, enteropathy, X-linked syndrome (IPEX) is caused by mutations of FOXP3. *Nat Genet*. Jan 2001;27(1):20-21.
 32. Brunkow ME, Jeffery EW, Hjerrild KA, et al. Disruption of a new forkhead/winged-helix protein, scurfin, results in the fatal

- lymphoproliferative disorder of the scurfy mouse. *Nat Genet.* Jan 2001;27(1):68-73.
33. Zhang L, Zhao Y. The regulation of Foxp3 expression in regulatory CD4(+)CD25(+)T cells: multiple pathways on the road. *J Cell Physiol.* Jun 2007;211(3):590-597.
 34. Fontenot JD, Gavin MA, Rudensky AY. Foxp3 programs the development and function of CD4+CD25+ regulatory T cells. *Nat Immunol.* Apr 2003;4(4):330-336.
 35. Gavin MA, Torgerson TR, Houston E, et al. Single-cell analysis of normal and FOXP3-mutant human T cells: FOXP3 expression without regulatory T cell development. *Proc Natl Acad Sci U S A.* Apr 25 2006;103(17):6659-6664.
 36. Bennett CL, Yoshioka R, Kiyosawa H, et al. X-Linked syndrome of polyendocrinopathy, immune dysfunction, and diarrhea maps to Xp11.23-Xq13.3. *Am J Hum Genet.* Feb 2000;66(2):461-468.
 37. Lopes JE, Soper DM, Ziegler SF. Foxp3 is required throughout the life of a regulatory T cell. *Sci STKE.* Jul 3 2007;2007(393):pe36.
 38. Baron U, Floess S, Wieczorek G, et al. DNA demethylation in the human FOXP3 locus discriminates regulatory T cells from activated FOXP3(+) conventional T cells. *Eur J Immunol.* Sep 2007;37(9):2378-2389.
 39. Egger G, Liang G, Aparicio A, Jones PA. Epigenetics in human disease and prospects for epigenetic therapy. *Nature.* May 27 2004;429(6990):457-463.
 40. Momparler RL, Bovenzi V. DNA methylation and cancer. *J Cell Physiol.* May 2000;183(2):145-154.
 41. Bird AP. CpG-rich islands and the function of DNA methylation. *Nature.* May 15-21 1986;321(6067):209-213.
 42. Wieczorek G, Asemussen A, Model F, et al. Quantitative DNA methylation analysis of FOXP3 as a new method for counting regulatory T cells in peripheral blood and solid tissue. *Cancer Res.* Jan 15 2009;69(2):599-608.
 43. Holschneider CH, Berek JS. Ovarian cancer: epidemiology, biology, and prognostic factors. *Semin Surg Oncol.* Jul-Aug 2000;19(1):3-10.
 44. Kolles H, Stegmaier C, von Seebach HB, Ziegler H. Deskriptive Epidemiologie und Prognose maligner gynakologischer Tumoren. *Geburtsh Frauenheilk.* 1989;49(06):573,578.
 45. du Bois A, Ewald-Riegler N, de Gregorio N, et al. Borderline tumours of the ovary: A cohort study of the Arbeitsgemeinschaft Gynakologische Onkologie (AGO) Study Group. *Eur J Cancer.* Mar 11 2013.
 46. Bergfeldt K, Rydh B, Granath F, et al. Risk of ovarian cancer in breast-cancer patients with a family history of breast or ovarian cancer: a population-based cohort study. *Lancet.* Sep 21 2002;360(9337):891-894.
 47. Gotlieb WH, Friedman E, Bar-Sade RB, et al. Rates of Jewish ancestral mutations in BRCA1 and BRCA2 in borderline ovarian tumors. *J Natl Cancer Inst.* Jul 1 1998;90(13):995-1000.
 48. Burger CW, Prinssen HM, Baak JP, Wagenaar N, Kenemans P. The management of borderline epithelial tumors of the ovary. *Int J Gynecol Cancer.* May 2000;10(3):181-197.

49. Whittemore AS, Harris R, Itnyre J. Characteristics relating to ovarian cancer risk: collaborative analysis of 12 US case-control studies. IV. The pathogenesis of epithelial ovarian cancer. Collaborative Ovarian Cancer Group. *Am J Epidemiol*. Nov 15 1992;136(10):1212-1220.
50. Parazzini F, Negri E, La Vecchia C, et al. Treatment for fertility and risk of ovarian tumors of borderline malignancy. *Gynecol Oncol*. Mar 1998;68(3):226-228.
51. Beral V, Doll R, Hermon C, Peto R, Reeves G. Ovarian cancer and oral contraceptives: collaborative reanalysis of data from 45 epidemiological studies including 23,257 women with ovarian cancer and 87,303 controls. *Lancet*. Jan 26 2008;371(9609):303-314.
52. Ness RB, Cramer DW, Goodman MT, et al. Infertility, fertility drugs, and ovarian cancer: a pooled analysis of case-control studies. *Am J Epidemiol*. Feb 1 2002;155(3):217-224.
53. Gertig DM, Hunter DJ, Cramer DW, et al. Prospective study of talc use and ovarian cancer. *J Natl Cancer Inst*. Feb 2 2000;92(3):249-252.
54. Ness RB, Grisso JA, Cottreau C, et al. Factors related to inflammation of the ovarian epithelium and risk of ovarian cancer. *Epidemiology*. Mar 2000;11(2):111-117.
55. Jordan SJ, Whiteman DC, Purdie DM, Green AC, Webb PM. Does smoking increase risk of ovarian cancer? A systematic review. *Gynecol Oncol*. Dec 2006;103(3):1122-1129.
56. Huncharek M, Kupelnick B. Dietary fat intake and risk of epithelial ovarian cancer: a meta-analysis of 6,689 subjects from 8 observational studies. *Nutr Cancer*. 2001;40(2):87-91.
57. Zhang M, Yang ZY, Binns CW, Lee AH. Diet and ovarian cancer risk: a case-control study in China. *Br J Cancer*. Mar 4 2002;86(5):712-717.
58. McCann SE, Moysich KB, Mettlin C. Intakes of selected nutrients and food groups and risk of ovarian cancer. *Nutr Cancer*. 2001;39(1):19-28.
59. Kushi LH, Mink PJ, Folsom AR, et al. Prospective study of diet and ovarian cancer. *Am J Epidemiol*. Jan 1 1999;149(1):21-31.
60. Bertone ER, Newcomb PA, Willett WC, Stampfer MJ, Egan KM. Recreational physical activity and ovarian cancer in a population-based case-control study. *Int J Cancer*. May 20 2002;99(3):431-436.
61. Pan SY, Ugnat AM, Mao Y. Physical activity and the risk of ovarian cancer: a case-control study in Canada. *Int J Cancer*. Nov 1 2005;117(2):300-307.
62. Olsen CM, Green AC, Whiteman DC, Sadeghi S, Kolaheer F, Webb PM. Obesity and the risk of epithelial ovarian cancer: a systematic review and meta-analysis. *Eur J Cancer*. Mar 2007;43(4):690-709.
63. Giordano ABA, and Kurman R. *Molecular Pathology of Gynecologic Cancer*. Vol 1: Human Press; 2007.
64. Denkert C, Dietel M. Borderline tumors of the ovary and peritoneal implants. *Verh Dtsch Ges Pathol*. 2005;89:84-91.
65. Sherman ME, Berman J, Birrer MJ, et al. Current challenges and opportunities for research on borderline ovarian tumors. *Hum Pathol*. Aug 2004;35(8):961-970.
66. Singer G, Oldt R, 3rd, Cohen Y, et al. Mutations in BRAF and KRAS characterize the development of low-grade ovarian serous carcinoma. *J Natl Cancer Inst*. Mar 19 2003;95(6):484-486.

67. Daly M, Oubrahim GI. Epidemiology and risk assessment for ovarian cancer. *Semin Oncol*. Jun 1998;25(3):255-264.
68. Kim TJ. Evolving strategies for ovarian cancer: gynecologic oncology in ASCO's 46th annual meeting. *J Gynecol Oncol*. Jun;21(2):72-74.
69. Van Calster B, Timmerman D, Bourne T, et al. Discrimination between benign and malignant adnexal masses by specialist ultrasound examination versus serum CA-125. *J Natl Cancer Inst*. Nov 21 2007;99(22):1706-1714.
70. Soper JT, Hunter VJ, Daly L, Tanner M, Creasman WT, Bast RC, Jr. Preoperative serum tumor-associated antigen levels in women with pelvic masses. *Obstet Gynecol*. Feb 1990;75(2):249-254.
71. EGTM. Tumour markers in gynaecological cancers - EGTM recommendations

. *European Group on Tumor Markers*

- 2009; http://www.egtm.eu/tumour_markers_in_gynaecological_cancers.htm.
72. Im SS, Gordon AN, Buttin BM, et al. Validation of referral guidelines for women with pelvic masses. *Obstet Gynecol*. Jan 2005;105(1):35-41.
 73. Classification and staging of malignant tumours in the female pelvis. *Acta Obstet Gynecol Scand*. 1971;50(1):1-7.
 74. Silverberg SG. Histopathologic grading of ovarian carcinoma: a review and proposal. *Int J Gynecol Pathol*. Jan 2000;19(1):7-15.
 75. Gershenson DM, Sun CC, Bodurka D, et al. Recurrent low-grade serous ovarian carcinoma is relatively chemoresistant. *Gynecol Oncol*. Jul 2009;114(1):48-52.
 76. Gershenson DM, Sun CC, Lu KH, et al. Clinical behavior of stage II-IV low-grade serous carcinoma of the ovary. *Obstet Gynecol*. Aug 2006;108(2):361-368.
 77. Hart WR. Borderline epithelial tumors of the ovary. *Mod Pathol*. Feb 2005;18 Suppl 2:S33-50.
 78. Burks RT, Sherman ME, Kurman RJ. Micropapillary serous carcinoma of the ovary. A distinctive low-grade carcinoma related to serous borderline tumors. *Am J Surg Pathol*. Nov 1996;20(11):1319-1330.
 79. Lee KR, Scully RE. Mucinous tumors of the ovary: a clinicopathologic study of 196 borderline tumors (of intestinal type) and carcinomas, including an evaluation of 11 cases with 'pseudomyxoma peritonei'. *Am J Surg Pathol*. Nov 2000;24(11):1447-1464.
 80. Hart WR, Norris HJ. Borderline and malignant mucinous tumors of the ovary. Histologic criteria and clinical behavior. *Cancer*. May 1973;31(5):1031-1045.
 81. Bell DA, Weinstock MA, Scully RE. Peritoneal implants of ovarian serous borderline tumors. Histologic features and prognosis. *Cancer*. Nov 15 1988;62(10):2212-2222.
 82. Koern J, Trope CG, Abeler VM. A retrospective study of 370 borderline tumors of the ovary treated at the Norwegian Radium Hospital from 1970 to 1982: a review of clinicopathologic features and treatment modalities. *Cancer*. 1993;1(71):1810-1820.
 83. Gershenson DM, Silva EG, Levy L, Burke TW, Wolf JK, Tornos C. Ovarian serous borderline tumors with invasive peritoneal implants. *Cancer*. Mar 15 1998;82(6):1096-1103.

84. Greene F, Balch C, Haller D, Morrow M. *AJCC Cancer Staging Manual (6th Edition)*: Springer; 2002.
85. Heintz AP, Odicino F, Maisonneuve P, et al. Carcinoma of the ovary. *J Epidemiol Biostat.* 2001;6(1):107-138.
86. Tinelli R, Tinelli A, Tinelli FG, Cicinelli E, Malvasi A. Conservative surgery for borderline ovarian tumors: a review. *Gynecol Oncol.* Jan 2006;100(1):185-191.
87. du Bois A, Rochon J, Pfisterer J, Hoskins WJ. Variations in institutional infrastructure, physician specialization and experience, and outcome in ovarian cancer: A systematic review. *Gynecologic Oncology.* 2009;112(2):422-436.
88. Mayer AR, Chambers SK, Graves E, et al. Ovarian cancer staging: Does it require a gynecologic oncologist? *Gynecologic Oncology.* 1992;47(2):223-227.
89. WEINSTEIN D, POLISHUK WZ. The Role of Wedge Resection of the Ovary As A Cause for Mechanical Sterility. *Obstetrical & Gynecological Survey.* 1976;31(3):227-228.
90. Crawford SC, Vasey PA, Paul J, Hay A, Davis JA, Kaye SB. Does aggressive surgery only benefit patients with less advanced ovarian cancer? Results from an international comparison within the SCOTROC-1 Trial. *J Clin Oncol.* Dec 1 2005;23(34):8802-8811.
91. du Bois A, Reuss A, Harter P, Pujade-Lauraine E, Ray-Coquard I, Pfisterer J. Potential role of lymphadenectomy in advanced ovarian cancer: a combined exploratory analysis of three prospectively randomized phase III multicenter trials. *J Clin Oncol.* Apr 1;28(10):1733-1739.
92. Querleu D, Papageorgiou T, Lambaudie E, Sonoda Y, Narducci F, LeBlanc E. Laparoscopic restaging of borderline ovarian tumours: results of 30 cases initially presumed as stage IA borderline ovarian tumours. *BJOG.* Feb 2003;110(2):201-204.
93. Trope CG, Kristensen G, Makar A. Surgery for borderline tumor of the ovary. *Semin Surg Oncol.* Jul-Aug 2000;19(1):69-75.
94. Fauvet R, Boccara J, Dufournet C, David-Montefiore E, Poncelet C, Darai E. Restaging surgery for women with borderline ovarian tumors: results of a French multicenter study. *Cancer.* Mar 15 2004;100(6):1145-1151.
95. Camatte S, Morice P, Thoury A, et al. Impact of surgical staging in patients with macroscopic "stage I" ovarian borderline tumours: analysis of a continuous series of 101 cases. *Eur J Cancer.* Aug 2004;40(12):1842-1849.
96. Trimble CL, Kosary C, Trimble EL. Long-term survival and patterns of care in women with ovarian tumors of low malignant potential. *Gynecol Oncol.* Jul 2002;86(1):34-37.
97. Seidman JD, Kurman RJ. Ovarian serous borderline tumors: a critical review of the literature with emphasis on prognostic indicators. *Hum Pathol.* May 2000;31(5):539-557.
98. Morice P, Camatte S, El Hassan J, Pautier P, Duvillard P, Castaigne D. Clinical outcomes and fertility after conservative treatment of ovarian borderline tumors. *Fertil Steril.* Jan 2001;75(1):92-96.
99. du Bois A, Luck H-J, Meier W, et al. A Randomized Clinical Trial of Cisplatin/Paclitaxel Versus Carboplatin/Paclitaxel as First-Line

- Treatment of Ovarian Cancer. *J. Natl. Cancer Inst.* September 3, 2003 2003;95(17):1320-1329.
100. Ozols RF, Bundy BN, Greer BE, et al. Phase III trial of carboplatin and paclitaxel compared with cisplatin and paclitaxel in patients with optimally resected stage III ovarian cancer: a Gynecologic Oncology Group study. *J Clin Oncol.* Sep 1 2003;21(17):3194-3200.
 101. Gadducci A, Sartori E, Landoni F, et al. Relationship Between Time Interval From Primary Surgery to the Start of Taxane- Plus Platinum-Based Chemotherapy and Clinical Outcome of Patients With Advanced Epithelial Ovarian Cancer: Results of a Multicenter Retrospective Italian Study. *J Clin Oncol.* February 1, 2005 2005;23(4):751-758.
 102. NIH consensus conference. Ovarian cancer. Screening, treatment, and follow-up. NIH Consensus Development Panel on Ovarian Cancer. *JAMA.* Feb 8 1995;273(6):491-497.
 103. Therasse P, Arbuck SG, Eisenhauer EA, et al. New guidelines to evaluate the response to treatment in solid tumors. European Organization for Research and Treatment of Cancer, National Cancer Institute of the United States, National Cancer Institute of Canada. *J Natl Cancer Inst.* Feb 2 2000;92(3):205-216.
 104. Guiot C, Degiorgis PG, Delsanto PP, Gabriele P, Deisboeck TS. Does tumor growth follow a "universal law"? *J Theor Biol.* Nov 21 2003;225(2):147-151.
 105. Morice P, Uzan C, Fauvet R, Gouy S, Duvillard P, Darai E. Borderline ovarian tumour: pathological diagnostic dilemma and risk factors for invasive or lethal recurrence. *Lancet Oncol.* Mar 2012;13(3):e103-115.
 106. Bell KA, Smith Sehdev AE, Kurman RJ. Refined diagnostic criteria for implants associated with ovarian atypical proliferative serous tumors (borderline) and micropapillary serous carcinomas. *Am J Surg Pathol.* Apr 2001;25(4):419-432.
 107. Noshok K, Baba Y, Tanaka N, et al. Tumour-infiltrating T-cell subsets, molecular changes in colorectal cancer, and prognosis: cohort study and literature review. *J Pathol.* Dec;222(4):350-366.
 108. Zhang L, Conejo-Garcia JR, Katsaros D, et al. Intratumoral T cells, recurrence, and survival in epithelial ovarian cancer. *N Engl J Med.* Jan 16 2003;348(3):203-213.
 109. Tomsova M, Melichar B, Sedlakova I, Steiner I. Prognostic significance of CD3+ tumor-infiltrating lymphocytes in ovarian carcinoma. *Gynecol Oncol.* Feb 2008;108(2):415-420.
 110. Schindl M, Schoppmann SF, Strobel T, et al. Level of Id-1 protein expression correlates with poor differentiation, enhanced malignant potential, and more aggressive clinical behavior of epithelial ovarian tumors. *Clin Cancer Res.* Feb 2003;9(2):779-785.
 111. Shen GH, Ghazizadeh M, Kawanami O, et al. Prognostic significance of vascular endothelial growth factor expression in human ovarian carcinoma. *Br J Cancer.* Jul 2000;83(2):196-203.
 112. Wolf M, Schimpl A, Hunig T. Control of T cell hyperactivation in IL-2-deficient mice by CD4(+)CD25(-) and CD4(+)CD25(+) T cells: evidence for two distinct regulatory mechanisms. *Eur J Immunol.* Jun 2001;31(6):1637-1645.
 113. Gobert M, Treilleux I, Bendriss-Vermare N, et al. Regulatory T cells recruited through CCL22/CCR4 are selectively activated in lymphoid

- infiltrates surrounding primary breast tumors and lead to an adverse clinical outcome. *Cancer Res.* Mar 1 2009;69(5):2000-2009.
114. Olkhanud PB, Baatar D, Bodogai M, et al. Breast cancer lung metastasis requires expression of chemokine receptor CCR4 and regulatory T cells. *Cancer Res.* Jul 15 2009;69(14):5996-6004.
 115. Haas J, Schopp L, Storch-Hagenlocher B, et al. Specific recruitment of regulatory T cells into the CSF in lymphomatous and carcinomatous meningitis. *Blood.* Jan 15 2008;111(2):761-766.
 116. Qin X-J, Shi H-Z, Deng J-M, Liang Q-L, Jiang J, Ye Z-J. CCL22 Recruits CD4-positive CD25-positive Regulatory T Cells into Malignant Pleural Effusion. *Clinical Cancer Research.* April 1, 2009 2009;15(7):2231-2237.
 117. Bates GJ, Fox SB, Han C, et al. Quantification of regulatory T cells enables the identification of high-risk breast cancer patients and those at risk of late relapse. *J Clin Oncol.* Dec 1 2006;24(34):5373-5380.
 118. Ikemoto T, Yamaguchi T, Morine Y, et al. Clinical roles of increased populations of Foxp3+CD4+ T cells in peripheral blood from advanced pancreatic cancer patients. *Pancreas.* Nov 2006;33(4):386-390.
 119. Fu J, Xu D, Liu Z, et al. Increased regulatory T cells correlate with CD8 T-cell impairment and poor survival in hepatocellular carcinoma patients. *Gastroenterology.* Jun 2007;132(7):2328-2339.
 120. Mizukami Y, Kono K, Kawaguchi Y, et al. Localisation pattern of Foxp3+ regulatory T cells is associated with clinical behaviour in gastric cancer. *Br J Cancer.* Jan 15 2008;98(1):148-153.
 121. Rodriguez GC, Haisley C, Hurteau J, et al. Regulation of invasion of epithelial ovarian cancer by transforming growth factor-beta. *Gynecol Oncol.* Feb 2001;80(2):245-253.
 122. Wei S, Kryczek I, Zou L, et al. Plasmacytoid dendritic cells induce CD8+ regulatory T cells in human ovarian carcinoma. *Cancer Res.* Jun 15 2005;65(12):5020-5026.
 123. Munn DH, Mellor AL. Indoleamine 2,3-dioxygenase and tumor-induced tolerance. *J Clin Invest.* May 2007;117(5):1147-1154.
 124. Sato E, Olson SH, Ahn J, et al. Intraepithelial CD8+ tumor-infiltrating lymphocytes and a high CD8+/regulatory T cell ratio are associated with favorable prognosis in ovarian cancer. *Proc Natl Acad Sci U S A.* Dec 20 2005;102(51):18538-18543.
 125. Gao Q, Qiu SJ, Fan J, et al. Intratumoral balance of regulatory and cytotoxic T cells is associated with prognosis of hepatocellular carcinoma after resection. *J Clin Oncol.* Jun 20 2007;25(18):2586-2593.
 126. Jordanova ES, Gorter A, Ayachi O, et al. Human leukocyte antigen class I, MHC class I chain-related molecule A, and CD8+/regulatory T-cell ratio: which variable determines survival of cervical cancer patients? *Clin Cancer Res.* Apr 1 2008;14(7):2028-2035.
 127. Petersen RP, Campa MJ, Sperlazza J, et al. Tumor infiltrating Foxp3+ regulatory T-cells are associated with recurrence in pathologic stage I NSCLC patients. *Cancer.* Dec 15 2006;107(12):2866-2872.

Statement of Responsibility

The general idea for this work originated from Professor Dr. med. Jalid Sehouli and Sven Olek, PhD. The concept and details were developed by Ines I.M. Vasconcelos.

All experiments (DNA extraction, bisulfite conversion and PCR amplification) regarding the epigenetic quantification of T-lymphocytes in epithelial ovarian tumors were performed by Ines I.M. Vasconcelos.

All the biostatistical analysis were performed by Ines I.M. Vasconcelos and supervised by Nora Galambos, PhD.

All the writing was done by Ines I.M. Vasconcelos.

Eidesstattliche Versicherung

„Ich, Ines Isabel Monteiro Vasconcelos versichere an Eides statt durch meine eigenhändige Unterschrift, dass ich die vorgelegte Dissertation mit dem Thema: “Epigenetic Quantification of Tumor-Infiltrating T-lymphocytes in Epithelial Ovarian Tumors” selbstständig und ohne nicht offengelegte Hilfe Dritter verfasst und keine anderen als die angegebenen Quellen und Hilfsmittel genutzt habe.

Alle Stellen, die wörtlich oder dem Sinne nach auf Publikationen oder Vorträgen anderer Autoren beruhen, sind als solche in korrekter Zitierung (siehe „Uniform Requirements for Manuscripts (URM)“ des ICMJE - www.icmje.org) kenntlich gemacht. Die Abschnitte zu Methodik (insbesondere praktische Arbeiten, Laborbestimmungen, statistische Aufarbeitung) und Resultaten (insbesondere Abbildungen, Graphiken und Tabellen) entsprechen den URM (s.o) und werden von mir verantwortet.

Meine Anteile an etwaigen Publikationen zu dieser Dissertation entsprechen denen, die in der untenstehenden gemeinsamen Erklärung mit dem/der Betreuer/in, angegeben sind. Sämtliche Publikationen, die aus dieser Dissertation hervorgegangen sind und bei denen ich Autor bin, entsprechen den URM (s.o) und werden von mir verantwortet.

Die Bedeutung dieser eidesstattlichen Versicherung und die strafrechtlichen Folgen einer unwahren eidesstattlichen Versicherung (§156,161 des Strafgesetzbuches) sind mir bekannt und bewusst.

Datum

01.07.2013

Unterschrift

Lebenslauf

"Mein Lebenslauf wird aus datenschutzrechtlichen Gründen in der elektronischen Version meiner Arbeit nicht veröffentlicht."

"Mein Lebenslauf wird aus datenschutzrechtlichen Gründen in der elektronischen Version meiner Arbeit nicht veröffentlicht."

"Mein Lebenslauf wird aus datenschutzrechtlichen Gründen in der elektronischen Version meiner Arbeit nicht veröffentlicht."

Publikationsliste

Türbachova I, Schwachula T, Vasconcelos I, Mustea A, Baldinger T, Gellhaus K, et al. The cellular ratio of immune tolerance (immunoCRIT) is a definite marker for aggressiveness of solid tumors and may explain tumor dissemination patterns. *Epigenetics* 2013; 8:19 - 18; PMID: 24071829; <http://dx.doi.org/10.4161/epi.26334> IF:4.58

CAVE: Erste Autorin! Geteilt Autorschaft: Türbachova, Schwachula und Vasconcelos

Vasconcelos I, Schoenegg W. Massive breast necrosis after extravasation of a full anthracycline cycle. *BMJ Case Rep* 2013. doi:10.1136/bcr-2013-201179 IF:17.22

Vasconcelos I, Olschewski J, Braicu EI, Sehouli J The impact of platinum-based adjuvant therapy on the outcome of borderline ovarian tumors: a systematic review and subgroup Meta-analysis. angenommen bei *PLOS One* am 01.2014 IF:3.73

Vasconcelos I, Siedentopf F, Frerichs O, Schoenegg W. An oncoplastic technique for the removal of large T3 central and upper located tumors in breast conserving therapy. eingereicht bei *Journal of Surgical Technique and Case Report* am 08.11.2013

Danksagung

Jalid Sehouli, Prof. Dr. med.

Sven Olek, PhD

Ioana Braicu, Dr. med.

Katharina Gellhaus, Dr. rer. nat.

Monika Menzel

Tatjana Cornu, Dr. rer. nat.

Tim Schwachula, Diplom. rer. nat.

Udo Baron, Dr. rer. nat.